Facultad de Ciencias Físico-Matemáticas
Universidad Michoacana de San Nicolás de Hidalgo

Computational Implementation and Statistical Analysis of Non-Standard Cosmological Models

Francisco Xavier Linares Cedeño

In collaboration with:
Ulises Nucamendi and Olivier Sarbach

Research-Oriented Colloquium
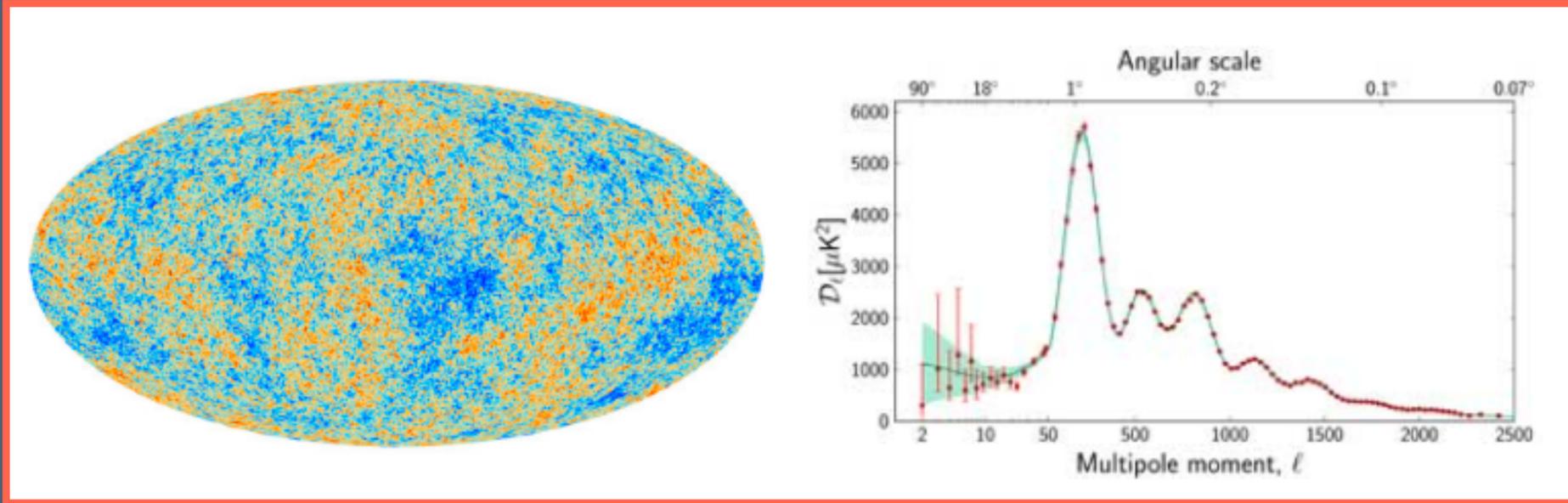Universidad de Deusto

Bilbao, 6 February, 2026

Pipeline
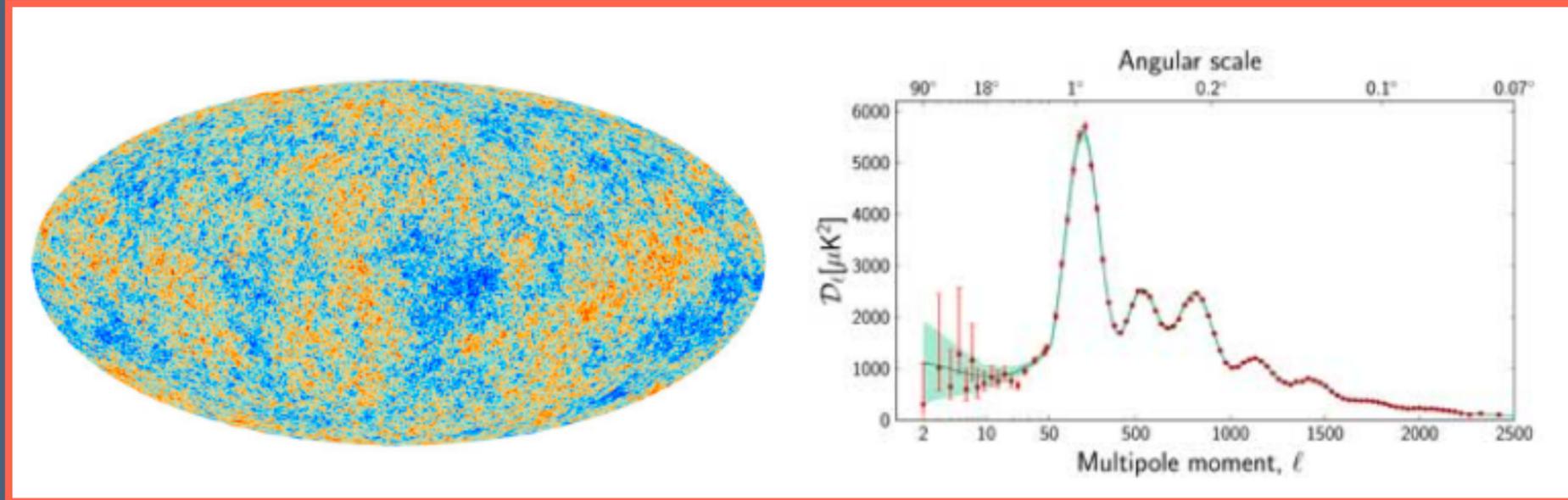
Pipeline

Pipeline

Theory: Temperature Power Spectrum

$$D_l = 2l(l+1) \int d^3k \; \mathscr{P}_\Psi(k) \; \Theta_l^2(k) \,.$$

Pipeline

Data: CMB anisotropies

Theory: Temperature Power Spectrum

$$D_l = 2l(l+1)\int d^3k \; \mathscr{P}_\Psi(k) \; \Theta_l^2(k).$$

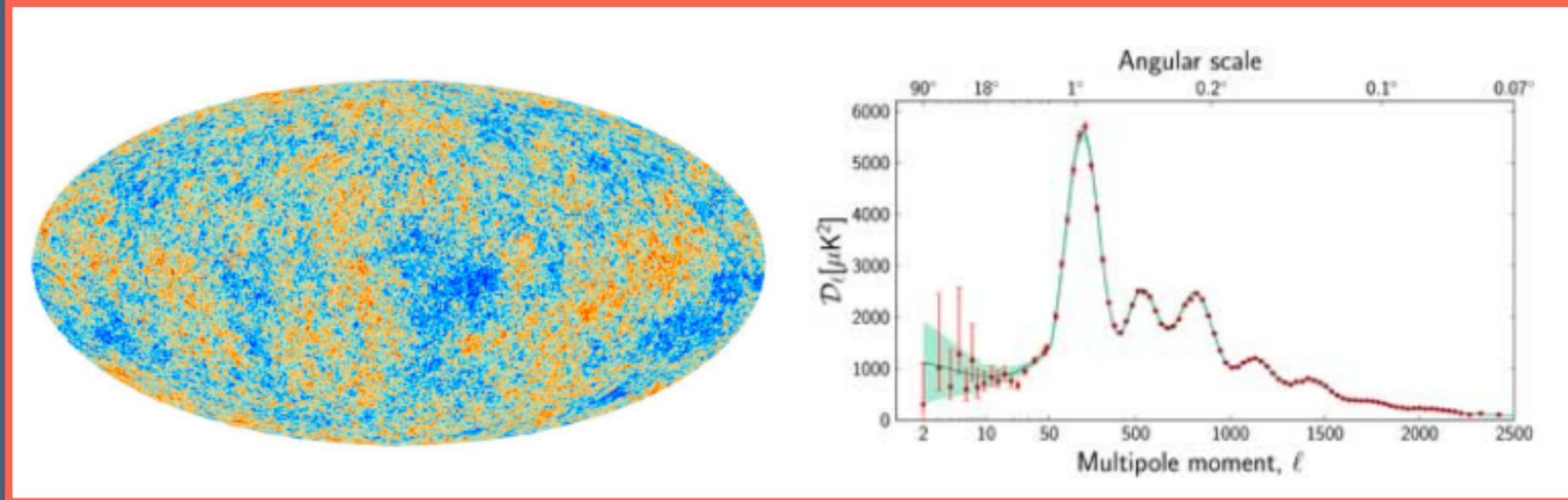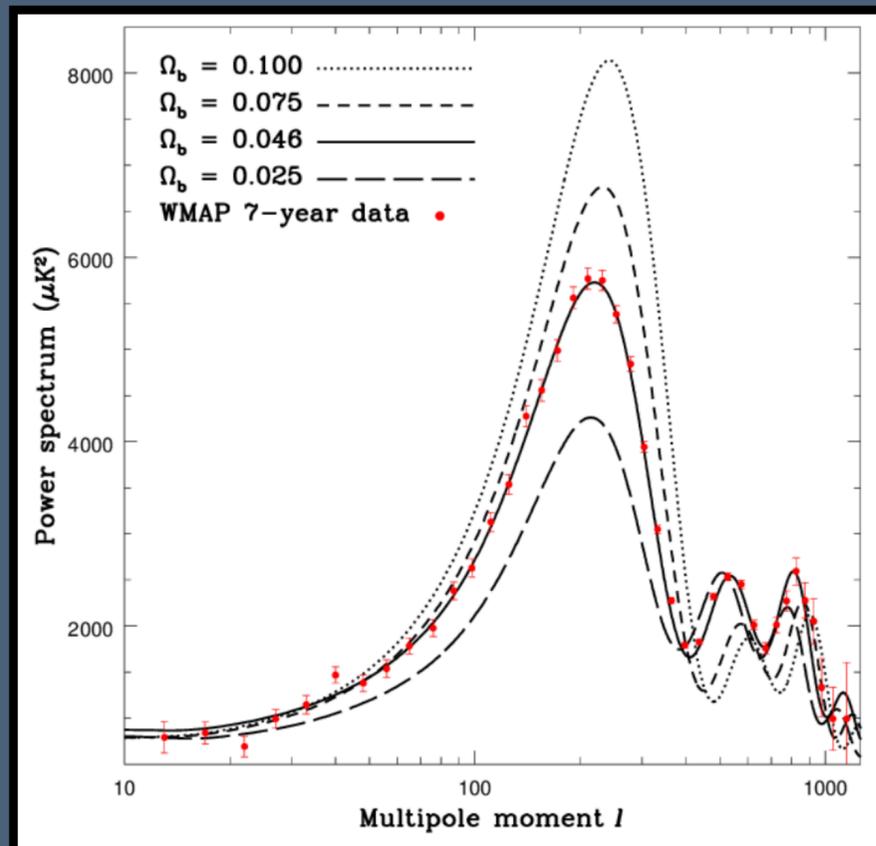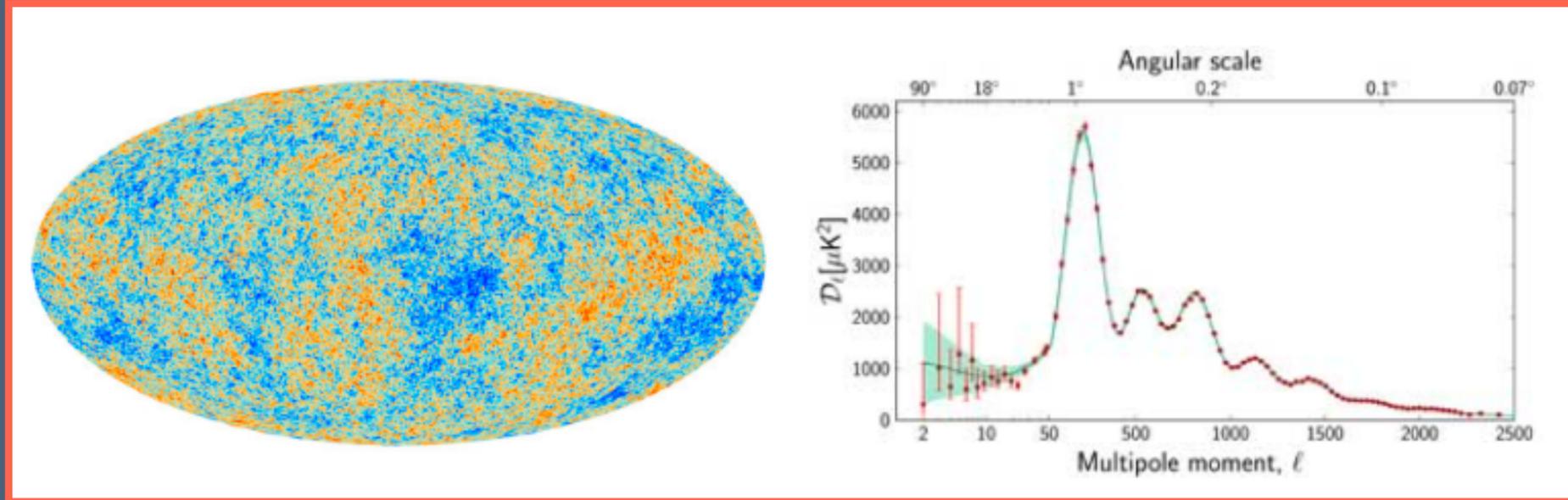## Data/Theory comparison

Pipeline

Data: CMB anisotropies

Theory: Temperature Power Spectrum

$$D_l = 2l(l+1) \int d^3k \; \mathscr{P}_{\Psi}(k) \; \Theta_l^2(k).$$

Prediction

Data/Theory comparison
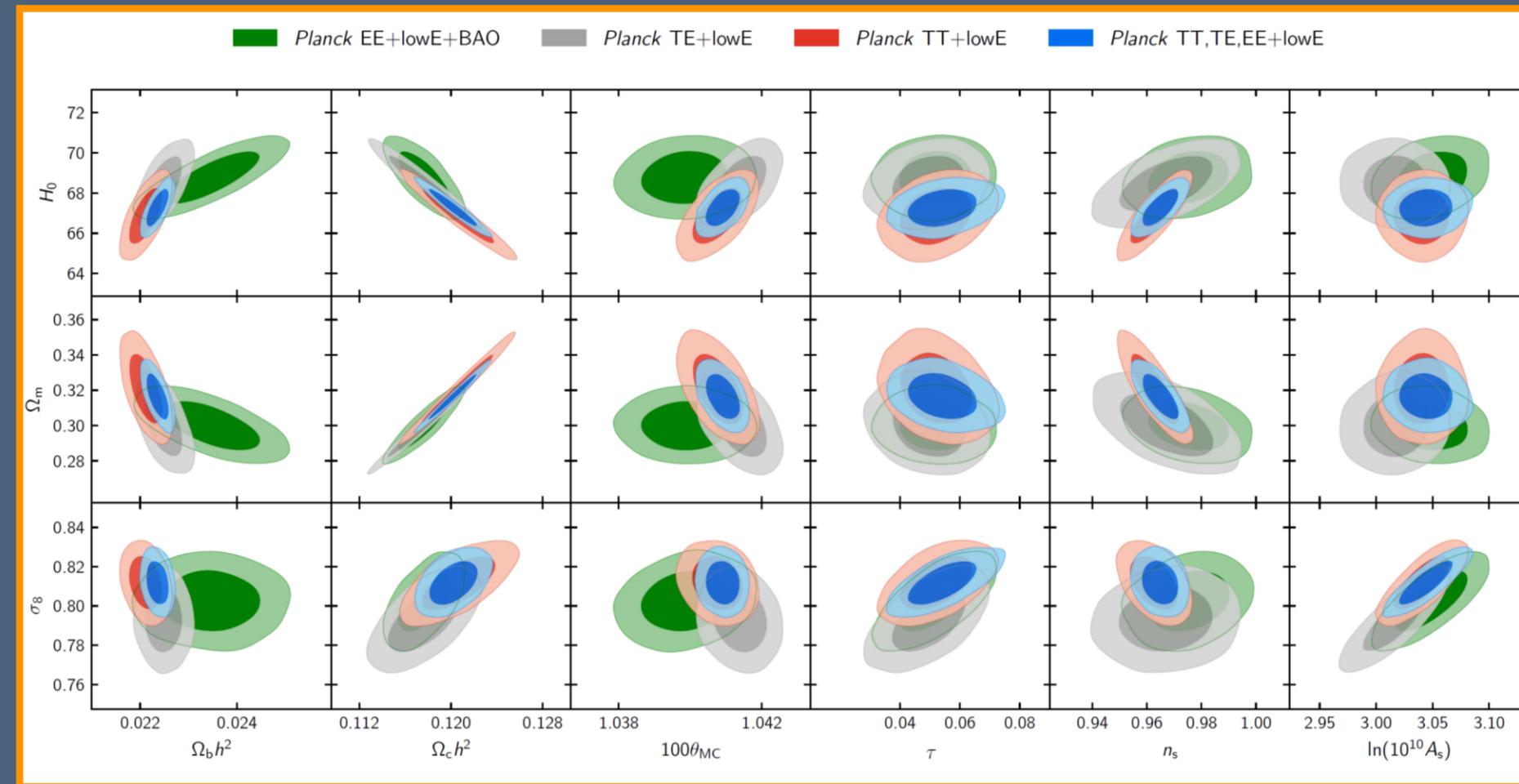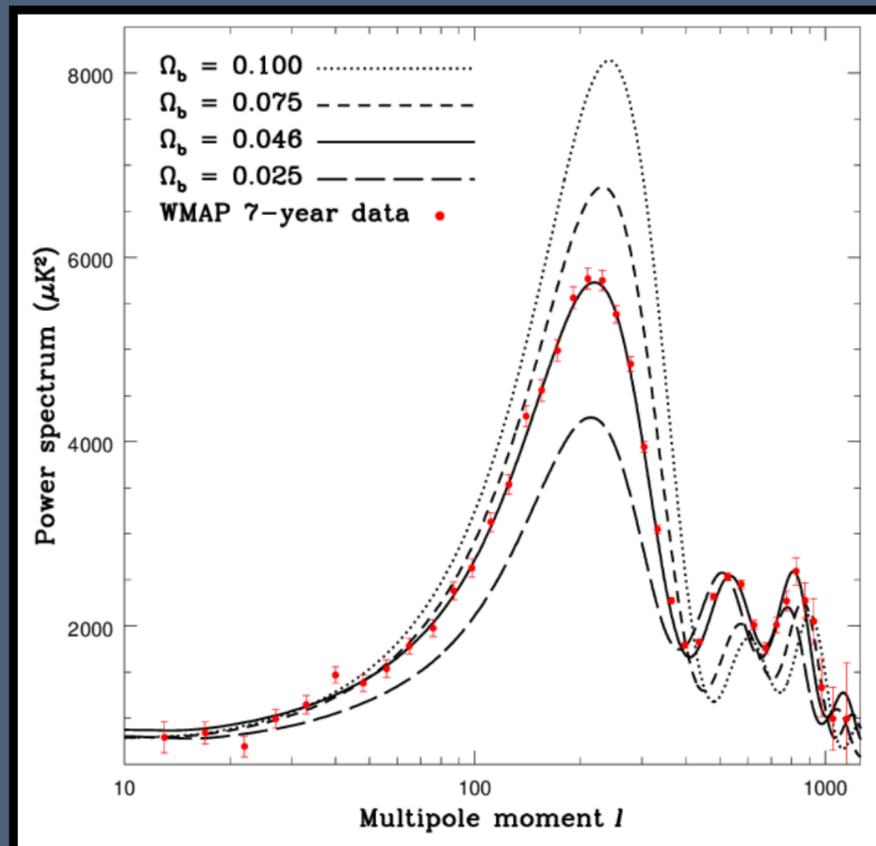
Data: (Likelihoods)

Public Planck Likelihood Code.
It provides C and Fortran libraries that allow users to compute the log likelihoods of the temperature maps.

http://pla.esac.esa.int/pla/#cosmology
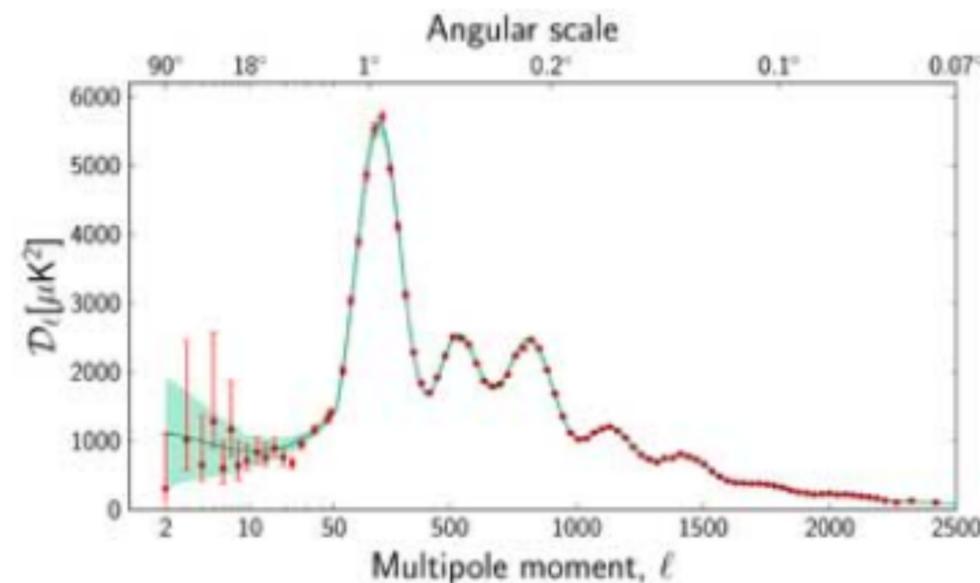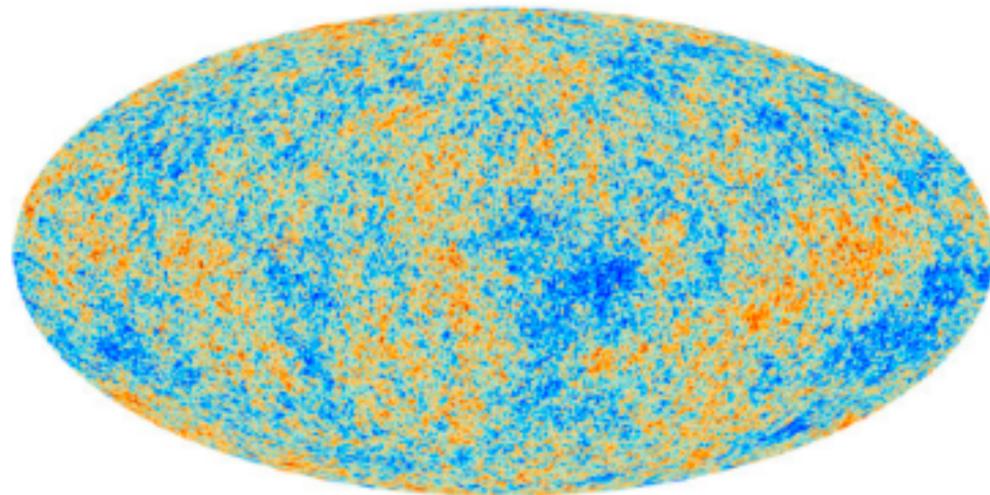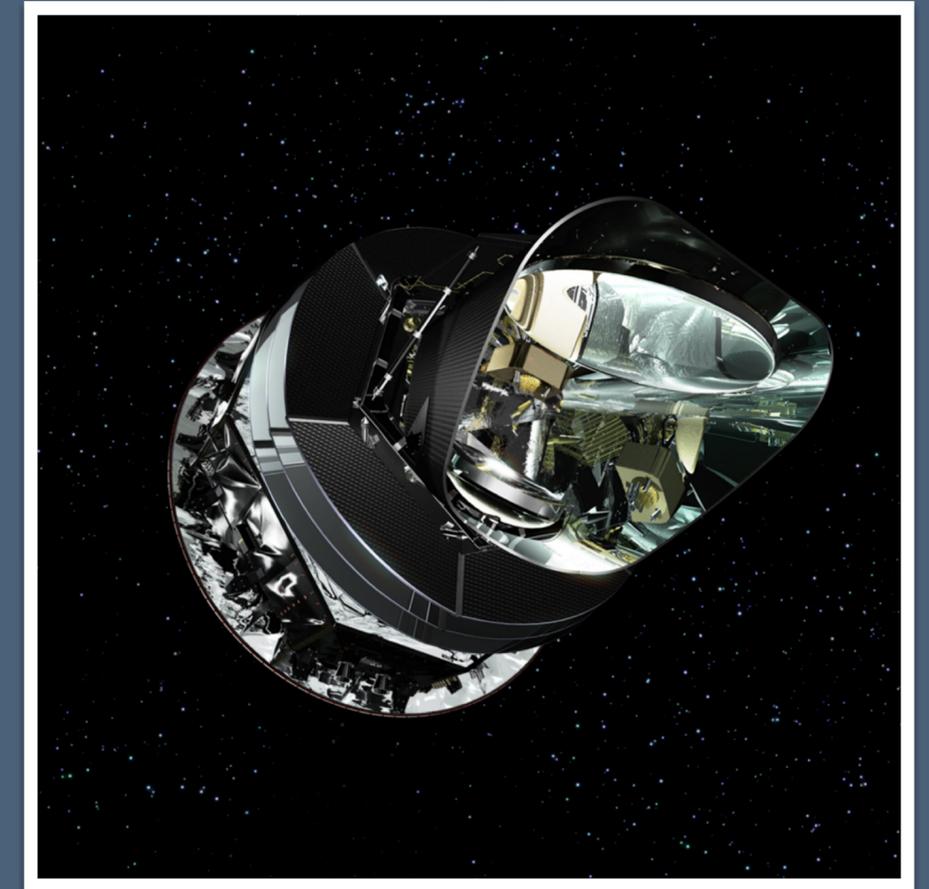
Installation instructions:

- C compiler, either gcc, clang or icc.
- fortran compiler, either ifort of gfortran
- **blas/lapack** library
- **cfitsio** library

Theoretical model: (GR + standard cosmological model ΛCDM)

$$H^2 = \frac{\kappa^2}{3}\bar\rho + \frac{\Lambda}{3}\,, \qquad \dot H = -\frac{\kappa^2}{2}\left(\bar\rho + p\right)\,, \qquad \dot{\bar\rho} + 3H(\bar\rho + p) = 0\,.$$

Background equations

Linear perturbation equations

$$\frac{\kappa^2}{2}(\delta\rho + 3\delta p + \nabla^2\pi^S) = \frac{\nabla^2\Phi}{a^2} + 3H\dot\Phi + 3\ddot\Psi + 6H\dot\Psi + 6(H^2 + \dot H)\Phi\,,$$

$$-\frac{\kappa^2}{2}(\bar\rho + \bar p)\partial_i v = H\partial_i\Phi + \partial_i\dot\Psi\,, \qquad \kappa^2 a^2\partial_i\partial_j\pi^S = \partial_i\partial_j(\Psi - \Phi)\,,$$

$$-\frac{\kappa^2}{2}(\delta\rho - \delta p - \nabla^2\pi^S) = H\dot\Phi + 2(3H^2 + \dot H)\Phi - \frac{\nabla^2\Psi}{a^2} + \ddot\Psi + 6H\dot\Psi\,.$$

Conservation equations

$$\dot{\delta\rho} + 3H(\delta\rho + \delta p) + \nabla^2\left[\frac{(\bar\rho + \bar p)}{a^2}v + H\pi^S\right] - 3(\bar\rho + \bar p)\dot\Psi = 0\,,$$

$$\delta p + \nabla^2\pi^S + \partial_t\left[(\bar\rho + \bar p)v\right] + 3H(\bar\rho + \bar p)v + (\bar\rho + \bar p)\Phi = 0\,.$$

Power Spectrum

$$D_l = 2l(l+1)\int d^3k \;\mathscr{P}_\Psi(k)\;\Theta_l^2(k)\,.$$

Data/Theory comparison: CLASS

Boltzmann Solver:

Cosmic Linear Anisotropy Solving System

CLASS

the Cosmic Linear Anisotropy Solving System

The purpose of CLASS is to simulate the evolution of linear perturbations in the universe and to compute CMB and large scale structure observables. CLASS also embeds several ways to compute non-linear corrections to linear perturbation theory. CLASS is written mainly in plain C, but with an original object-oriented style mimicking the notion of class. Since v3.2.3, some modules are actually compiled as C++, to handle the parallelisation of loops in the C++ way. The whole code is wrapped in the python module classy.

We hope that you will enjoy the use of CLASS,

Julien Lesgourgues, Nils Schöneberg, Thomas Tram

> Download
> Documentation
> Papers
> Versions
> Support

○ http://class-code.net/

○ https://github.com/lesgourg/class_public

class_public / source / **background.c**   ↑ Top

Code | Blame   Raw

```
650        /**
651         * Single place where the fluid equation of state is
652         * defined. Parameters of the function are passed through the
653         * background structure. Generalisation to arbitrary functions should
654         * be simple.
655         *
656         * @param pba           Input: pointer to background structure
657         * @param a             Input: current value of scale factor (in fact, with our conventions, of
658         * @param w_fld         Output: equation of state parameter w_fld(a)
659         * @param dw_over_da_fld Output: function dw_fld/da
660         * @param integral_fld   Output: function \f$ \int_{a}^{a_0} da 3(1+w_{fld})/a \f$
661         * @return the error status
662         */
663
664   ∨   int background_w_fld(
665                          struct background * pba,
666                          double a,
667                          double * w_fld,
668                          double * dw_over_da_fld,
669                          double * integral_fld
670                          ) {
671
672        double Omega_ede = 0.;
673        double dOmega_ede_over_da = 0.;
674        double d2Omega_ede_over_da2 = 0.;
675        double a_eq, Omega_r, Omega_m;
676
677        /** - first, define the function w(a) */
```

Data/Theory comparison: CLASS

Cosmological evolution of scalar field dark matter in the CLASS code: Accuracy and precision of numerical solutions

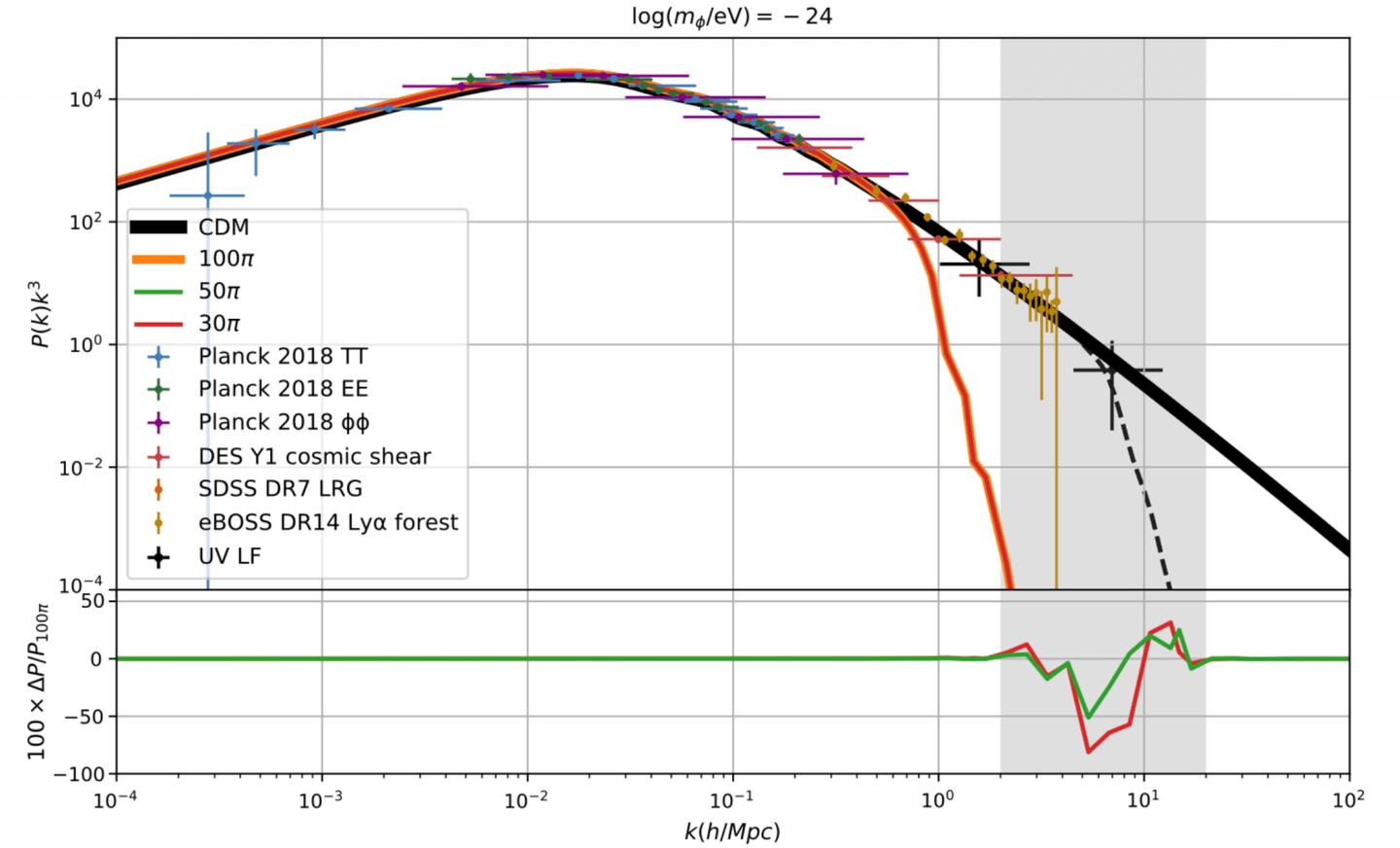L. Arturo Ureña-López[1,*] and Francisco X. Linares Cedeño[2,†]

[1]Departamento de Física, DCI, Campus León, Universidad de Guanajuato, 37150, León, Guanajuato, México

[2]Instituto de Física y Matemáticas, Universidad Michoacana de San Nicolás de Hidalgo, Edificio C-3, Ciudad Universitaria, CP. 58040 Morelia, Michoacán, México
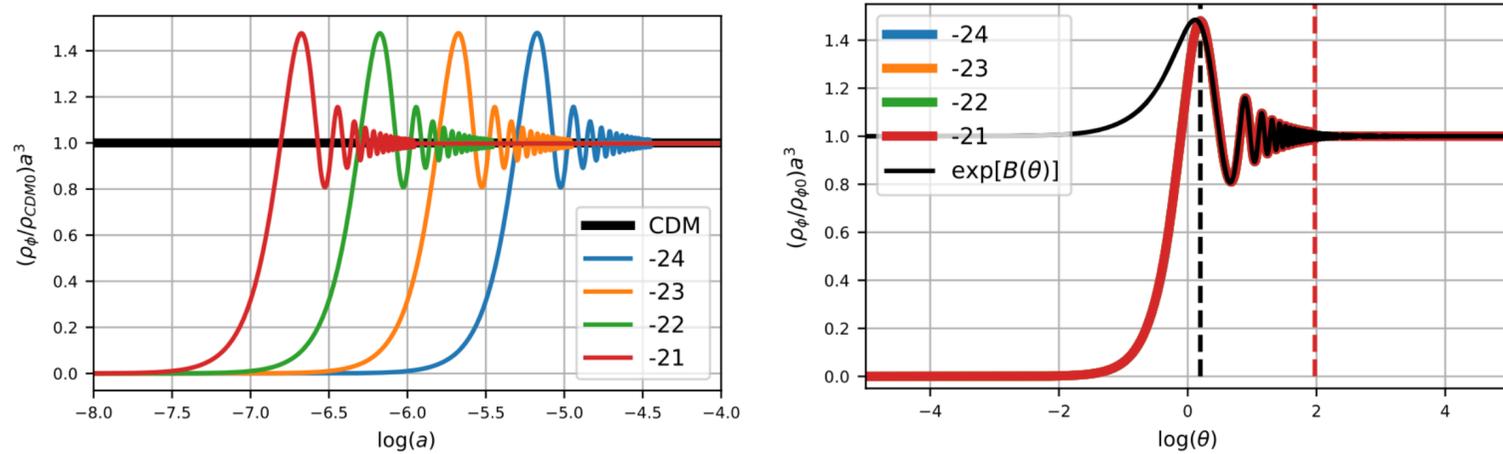
FIG. 3. Numerical solutions of the scalar field energy density ρ_ϕ, in a combination that highlights the asymptotic, nonoscillatory value at late times; the curves represent the same cases as in Fig. 1. Left: the energy density, as a function of the scale factor a, behaves as a pressureless component from the onset of rapid oscillations, which occur at times that depend on the field mass m_ϕ, but the late-time behavior is the same: decaying oscillations around a fixed value. The cutoff value was set at $\theta_\star = 30\pi$ for the four cases. Right: if plotted as a function of the polar angle θ, all curves collapse into a single one. Also shown is the semianalytical formula (33), with $B(\theta) \equiv 3\sin\theta/(\theta + 3\pi/4)$ (black curve), which is in good agreement with the numerical solutions from the start of the rapid oscillations at $\theta_{osc} = \pi/2$ (black dashed line). The cutoff value $\theta_\star = 30\pi$ (red dashed line) is also shown as a reference. See the text for more details.
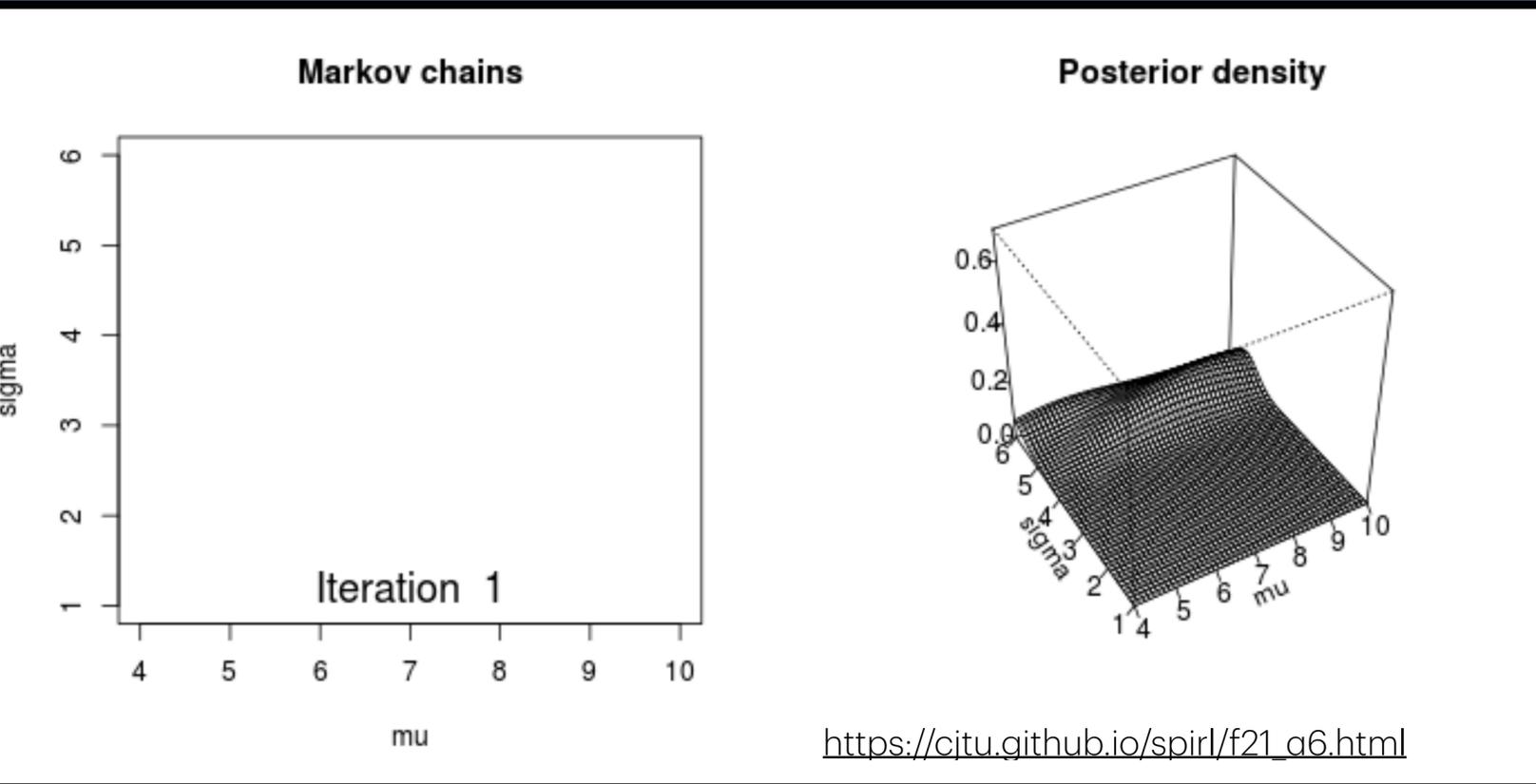
$$\theta' = -3\sin\theta + y_1, \quad y_1' = \frac{3}{2}\left(1 + w_{tot}\right)y_1 + \frac{\lambda}{2}\Omega_\phi\sin\theta, \quad \Omega_\phi' = 3(w_{tot} - w_\phi)\Omega_\phi.$$

$$\delta_0' = \left[-3\sin\theta - \frac{k^2}{k_J^2}(1 - \cos\theta)\right]\delta_1 + \frac{k^2}{k_J^2}\sin\theta\delta_0 - \frac{\bar{h}'}{2}(1 - \cos\theta),$$

$$\delta_1' = \left[-3\cos\theta - \frac{k_{eff}^2}{k_J^2}\sin\theta\right]\delta_1 + \frac{k_{eff}^2}{k_J^2}(1 + \cos\theta)\,\delta_0 - \frac{\bar{h}'}{2}\sin\theta.$$

Prediction: Monte Python
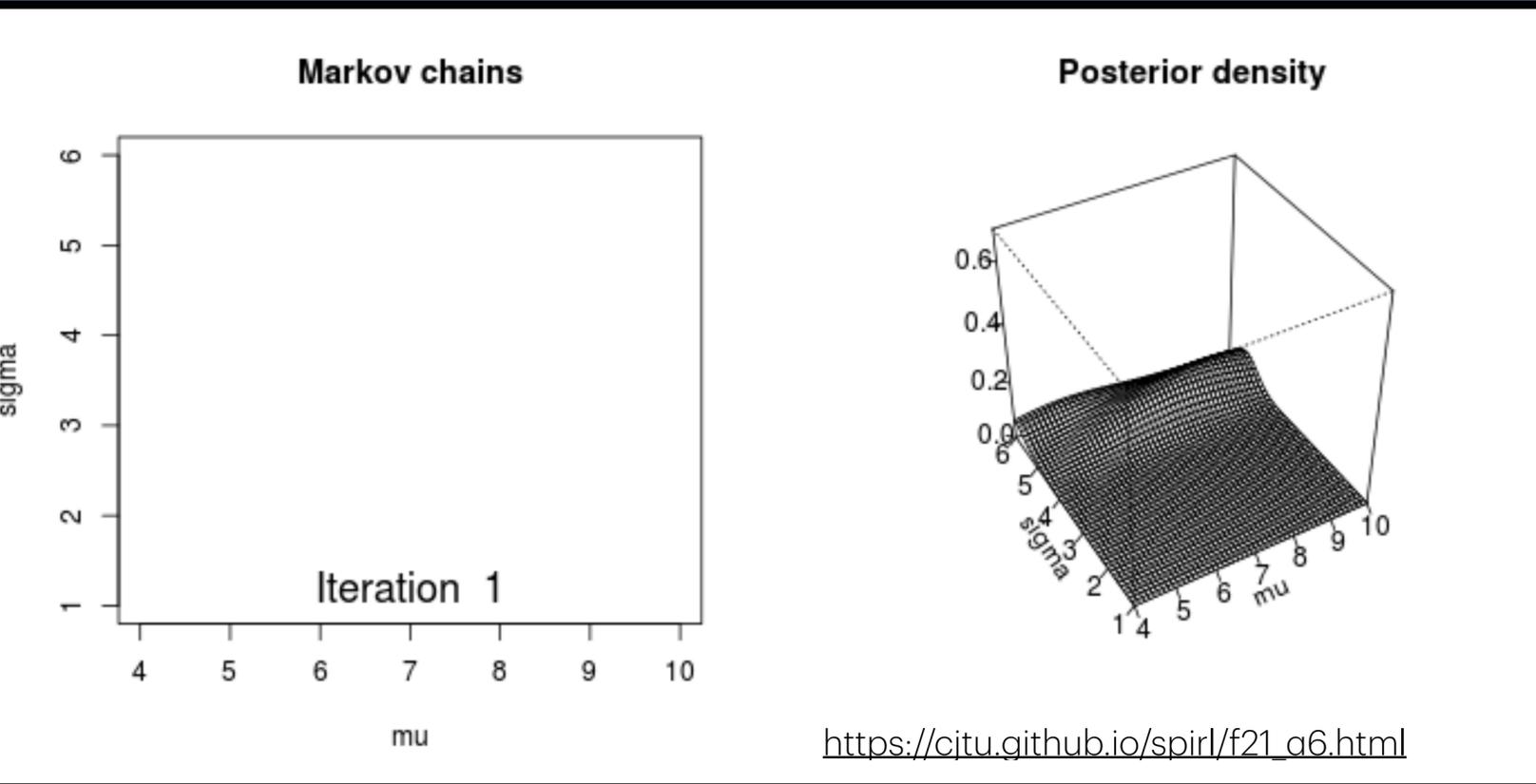
Markov Chain Monte Carlo (MCMC)

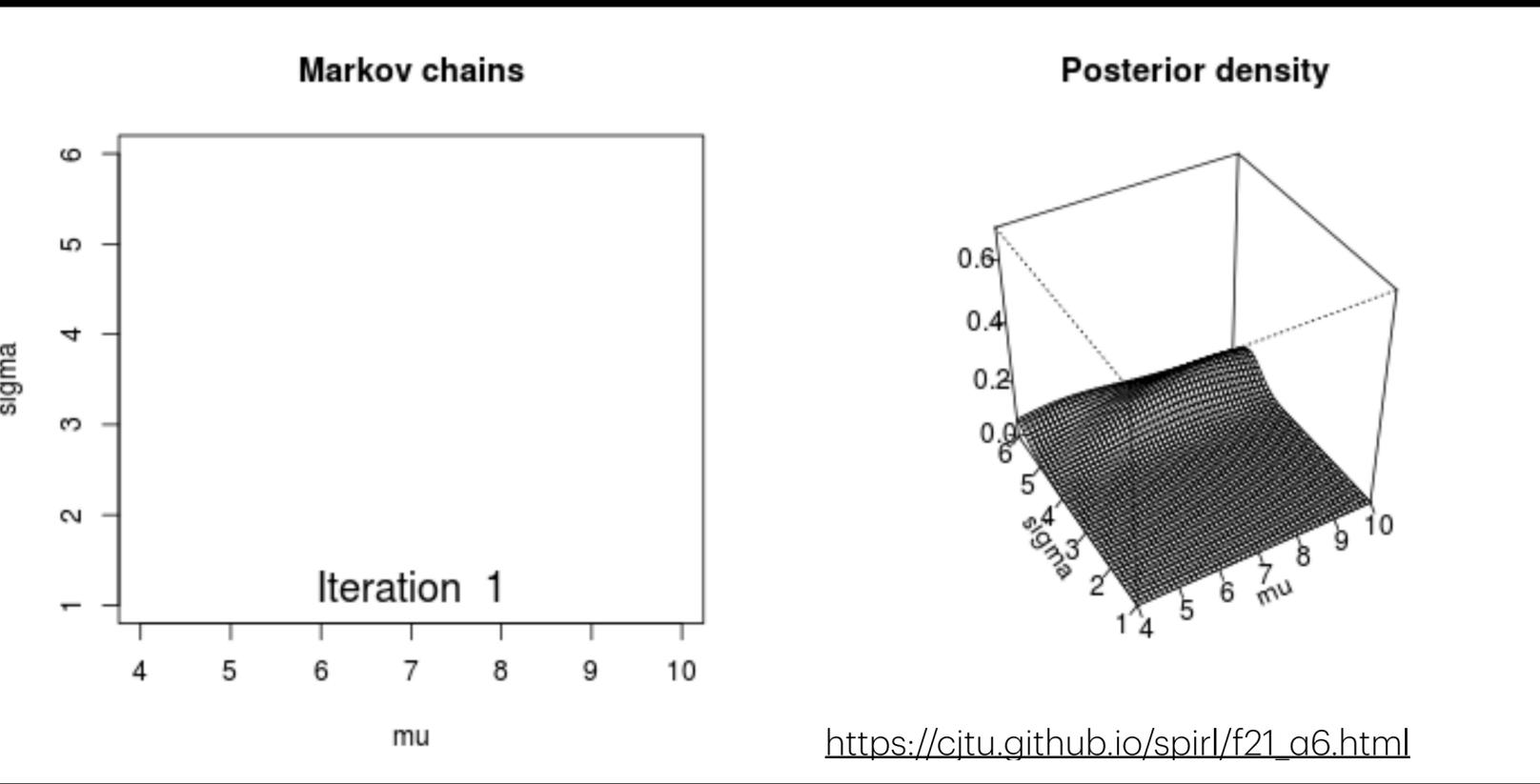https://cjtu.github.io/spirl/f21_a6.html

Prediction: Monte Python

Markov Chain Monte Carlo (MCMC)

https://cjtu.github.io/spirl/f21_a6.html

Prediction: Monte Python

Markov Chain Monte Carlo (MCMC)

Markov chains

Posterior density

Iteration 1

https://cjtu.github.io/spirl/f21_a6.html

Bayes's theorem

$$\mathscr{P}(\Theta \mid D, M) = \frac{\mathscr{L}(D \mid \Theta, M)\,\Pi(\Theta \mid M)}{\mathscr{E}(D \mid M)}$$

Prediction: Monte Python

Markov Chain Monte Carlo (MCMC)

https://cjtu.github.io/spirl/f21_a6.html
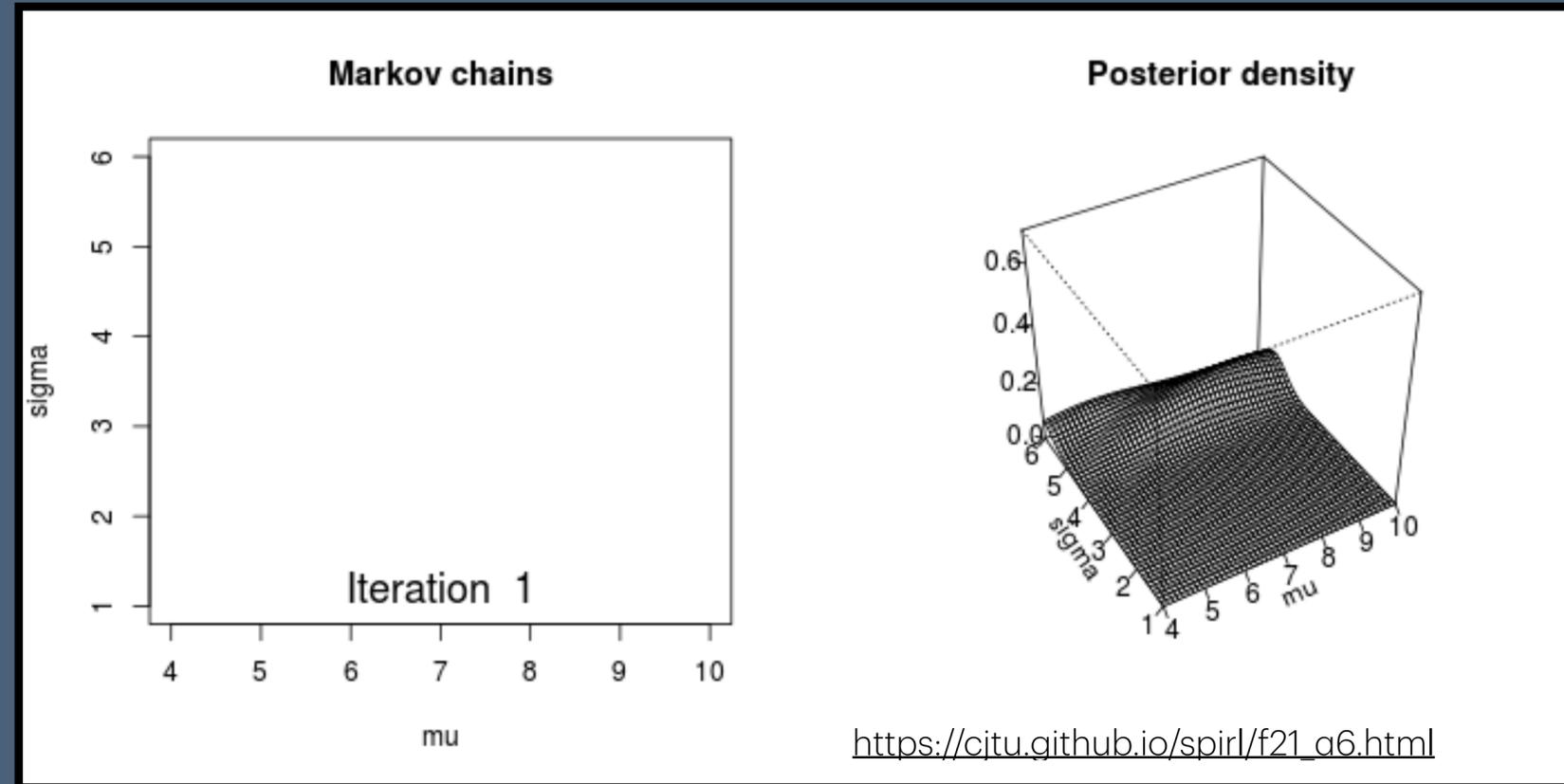
Bayes's theorem

$$\mathscr{P}(\Theta \mid D, M) = \frac{\mathscr{L}(D \mid \Theta, M) \, \Pi(\Theta \mid M)}{\mathscr{E}(D \mid M)}$$
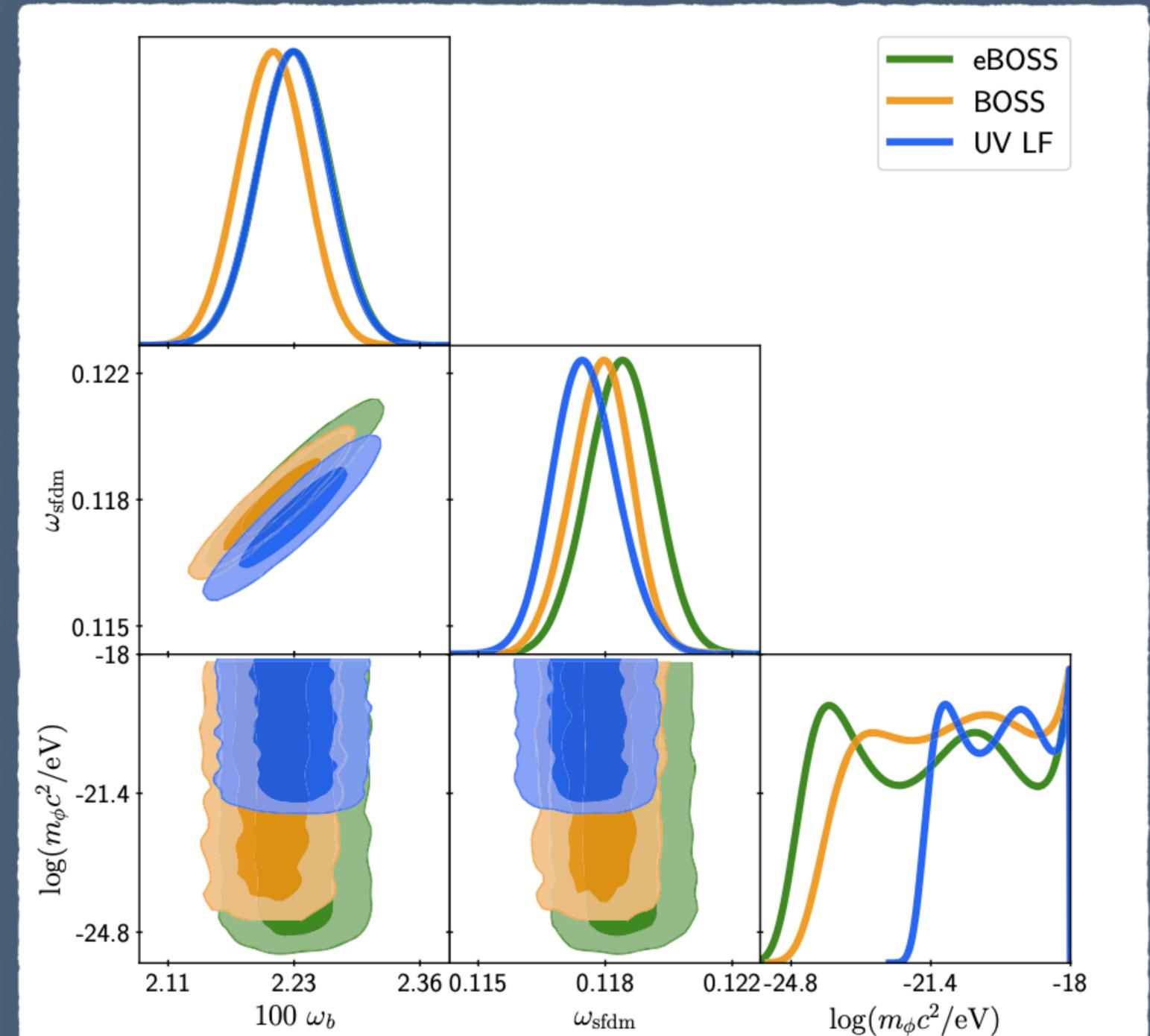
Prediction: Evidence & Bayes Factor

Journal of Cosmology and Astroparticle Physics
An IOP and SISSA journal

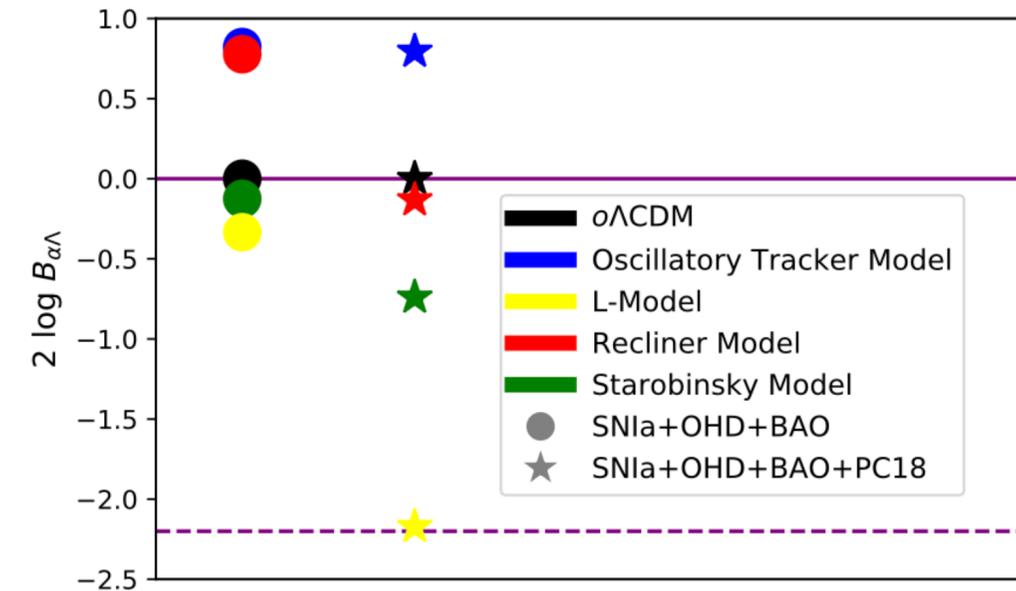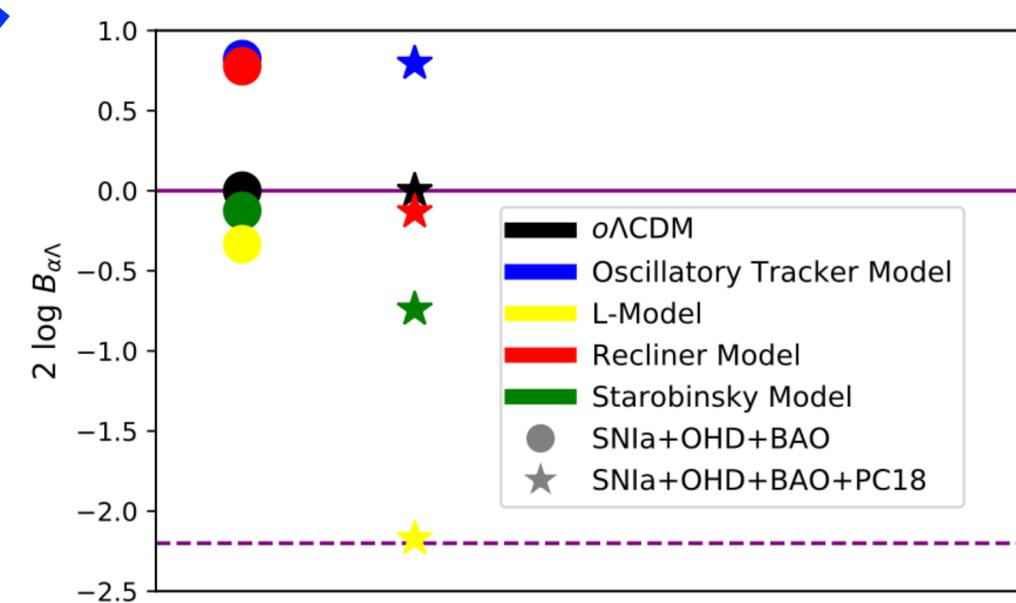### Bayesian evidence for α-attractor dark energy models

Francisco X. Linares Cedeño,[a,b,1] **Ariadna Montiel,**[b]
Juan Carlos Hidalgo[b] **and Gabriel German**[b]

Bayes's theorem

$$\mathscr{P}(\Theta \mid D, M) = \frac{\mathcal{L}(D \mid \Theta, M)\, \Pi(\Theta \mid M)}{\mathcal{E}(D \mid M)}$$

Potential	Local Obs		Local Obs+PC2018	
	$\log \mathcal{E}$	$2\log B$	$\log \mathcal{E}$	$2\log B$
$o\Lambda$CDM	-528.30	0	-542.29	0
L-model	-528.47	-0.33	-543.37	-2.17
Oscillatory tracker model	-527.89	0.82	-541.89	0.80
Recliner model	-527.92	0.78	-542.35	-0.13
Starobinsky model	-528.37	-0.13	-542.66	-0.74

Table 4. Evidences and Bayes factor for the different α-attractor potentials. The first two columns are the results obtained when considering only local observations (SNe Ia+OHD+BAO), whereas the last two columns show the results once adding the Planck Compressed 2018 (PC2018) data.

Figure 3. Bayes factor ($\log B$) for the comparison between the α-attractor models and ΛCDM. The first column with circles corresponds to the Bayes factor considering only local observations (SNe Ia+OHD+BAO), whereas the second column with stars indicate the Bayes factor once the Planck Compressed 2018 (PC2018) data were included. The horizontal purple solid (dashed) line labels the zero (-2.2) in the Jeffrey's scale according to table 2.

Prediction: Evidence & Bayes Factor

Bayesian evidence for α-attractor dark energy models

Francisco X. Linares Cedeño,[a,b,1] Ariadna Montiel,[b]
Juan Carlos Hidalgo[b] and Gabriel German[b]

Potential	Local Obs		Local Obs+PC2018	
	$\log \mathcal{E}$	$2\log B$	$\log \mathcal{E}$	$2\log B$
$o\Lambda$CDM	-528.30	0	-542.29	0
L-model	-528.47	-0.33	-543.37	-2.17
Oscillatory tracker model	-527.89	0.82	-541.89	0.80
Recliner model	-527.92	0.78	-542.35	-0.13
Starobinsky model	-528.37	-0.13	-542.66	-0.74

Table 4. Evidences and Bayes factor for the different α-attractor potentials. The first two columns are the results obtained when considering only local observations (SNe Ia+OHD+BAO), whereas the last two columns show the results once adding the Planck Compressed 2018 (PC2018) data.

Figure 3. Bayes factor ($\log B$) for the comparison between the α-attractor models and ΛCDM. The first column with circles corresponds to the Bayes factor considering only local observations (SNe Ia+OHD+BAO), whereas the second column with stars indicate the Bayes factor once the Planck Compressed 2018 (PC2018) data were included. The horizontal purple solid (dashed) line labels the zero (-2.2) in the Jeffrey's scale according to table 2.

Bayes's theorem

$$\mathscr{P}(\Theta \mid D, M) = \frac{\mathscr{L}(D \mid \Theta, M)\, \Pi(\Theta \mid M)}{\mathscr{E}(D \mid M)}$$

Prediction: Neural Network with Harmonic

https://astro-informatics.github.io/harmonic/

Evidence

$$\mathscr{E}(D \mid M) = \int d\Theta \; \mathscr{L}(D \mid \Theta, M) \; \Pi(\Theta \mid M).$$

Multidimensional integral → highly involving and time consuming.

Prediction: Neural Network with Harmonic

https://astro-informatics.github.io/harmonic/

Evidence

$$\mathcal{E}(D \mid M) = \int d\Theta \; \mathcal{L}(D \mid \Theta, M) \; \Pi(\Theta \mid M).$$

Multidimensional integral $\rightarrow$ highly involving and time consuming.

Evidence:
Harmonic Mean Estimator

$$\mathcal{E}_{HME} = \left[\frac{1}{N} \sum_{i=1}^{N} \frac{1}{\mathcal{L}(\Theta_i)} \right]^{-1}$$

Prediction: Neural Network with Harmonic

https://astro-informatics.github.io/harmonic/

Evidence

$$\mathcal{E}(D \mid M) = \int d\Theta \; \mathcal{L}(D \mid \Theta, M) \; \Pi(\Theta \mid M).$$

Multidimensional integral → highly involving and time consuming.

Evidence: Harmonic Mean Estimator

$$\mathcal{E}_{HME} = \left[\frac{1}{N} \sum_{i=1}^{N} \frac{1}{\mathcal{L}(\Theta_i)} \right]^{-1}$$

Evidence: Learnt Harmonic Mean Estimator

$$\mathcal{E}_{LHME} = \left[\frac{1}{N} \sum_{i=1}^{N} \frac{h(\Theta_i)}{\mathcal{L}(\Theta_i)\pi(\Theta_i)} \right]^{-1}$$

Prediction: Neural Network with Harmonic

https://astro-informatics.github.io/harmonic/

Evidence

$$\mathcal{E}(D \mid M) = \int d\Theta \; \mathcal{L}(D \mid \Theta, M) \; \Pi(\Theta \mid M).$$

Multidimensional integral → highly involving and time consuming.

**Evidence:
Harmonic Mean Estimator**

$$\mathcal{E}_{HME} = \left[\frac{1}{N} \sum_{i=1}^{N} \frac{1}{\mathcal{L}(\Theta_i)} \right]^{-1}$$

Neural Networks used to obtain $h(\Theta_i)$

**Evidence:
Learnt Harmonic Mean Estimator**

$$\mathcal{E}_{LHME} = \left[\frac{1}{N} \sum_{i=1}^{N} \frac{h(\Theta_i)}{\mathcal{L}(\Theta_i)\pi(\Theta_i)} \right]^{-1}$$

Our aim is to explore whether this relativistic kinetic gas leads to a consistent cosmological evolution for the dark matter component, even when it behaves relativistically at early times.

Our aim is to explore whether this relativistic kinetic gas leads to a consistent cosmological evolution for the dark matter component, even when it behaves relativistically at early times.

The dynamics of a spatially flat FLRW universe is given by:
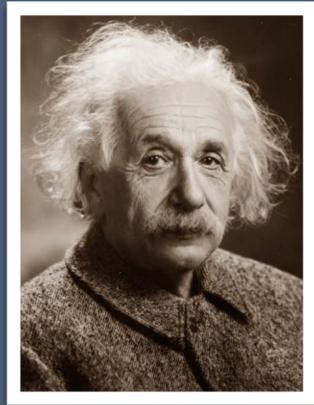
$$G_{\mu\nu} + \Lambda g_{\mu\nu} = \kappa^2 T_{\mu\nu} \longrightarrow \begin{cases} H^2 = \dfrac{\kappa^2}{3}\left(\dfrac{\rho_{0,b}}{a^3} + \dfrac{\rho_{0,r}}{a^4} + \dfrac{\rho_{0,DM}}{a^4}\sqrt{\dfrac{a^2 + \beta^2}{1 + \beta^2}} + \rho_\Lambda \right), \\[4mm] \dot{H} = -\dfrac{\kappa}{2}\left[\rho_b(1 + \omega_b) + \rho_r(1 + \omega_r) + \rho_{DM}(1 + \omega_{DM}) \right]. \end{cases}$$

The conservation of the energy-momentum tensor gives:

$$\dot{\rho}_b = -3H\rho_b(1 + \omega_b)\,, \qquad \dot{\rho}_r = -3H\rho_r(1 + \omega_r)\,, \qquad \dot{\rho}_{DM} = -3H\rho_{DM}(1 + \omega_{DM})\,.$$
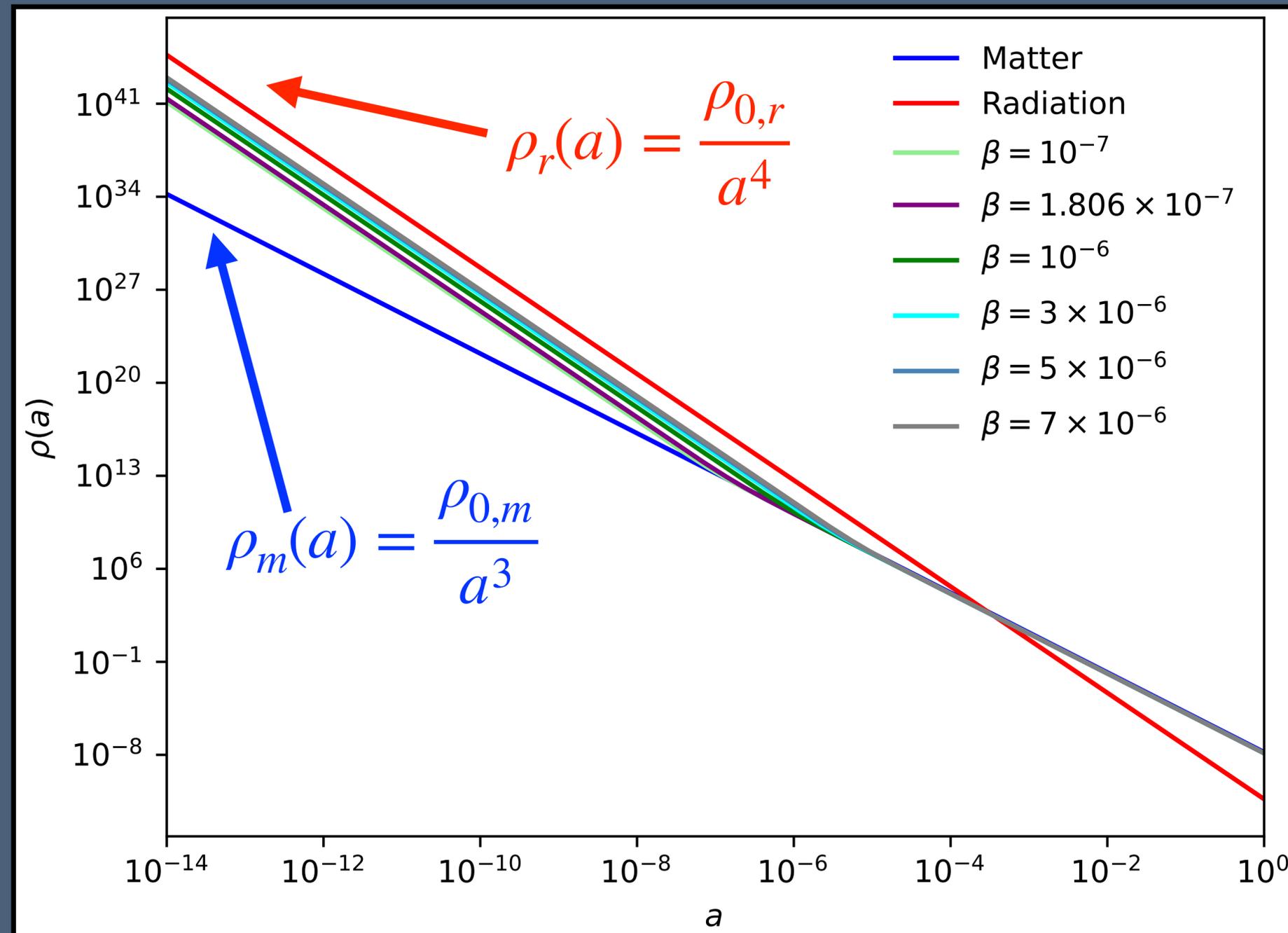
$$\rho_{DM}(a) = \frac{\rho_0}{a^4}\sqrt{\frac{a^2 + \beta^2}{1 + \beta^2}}\,.$$

$$\rho_{DM}(a) = \begin{cases} \rho_{0,DM}/a^4\,, & \text{at early times}\,. \\ \rho_{0,DM}/a^3\,, & \text{at late times}\,. \end{cases}$$

Figure legend:
- Matter
- Radiation
- $\beta = 10^{-7}$
- $\beta = 1.806 \times 10^{-7}$
- $\beta = 10^{-6}$
- $\beta = 3 \times 10^{-6}$
- $\beta = 5 \times 10^{-6}$
- $\beta = 7 \times 10^{-6}$

$$\rho_r(a) = \frac{\rho_{0,r}}{a^4}$$

$$\rho_m(a) = \frac{\rho_{0,m}}{a^3}$$

Comparison with Neutrinos
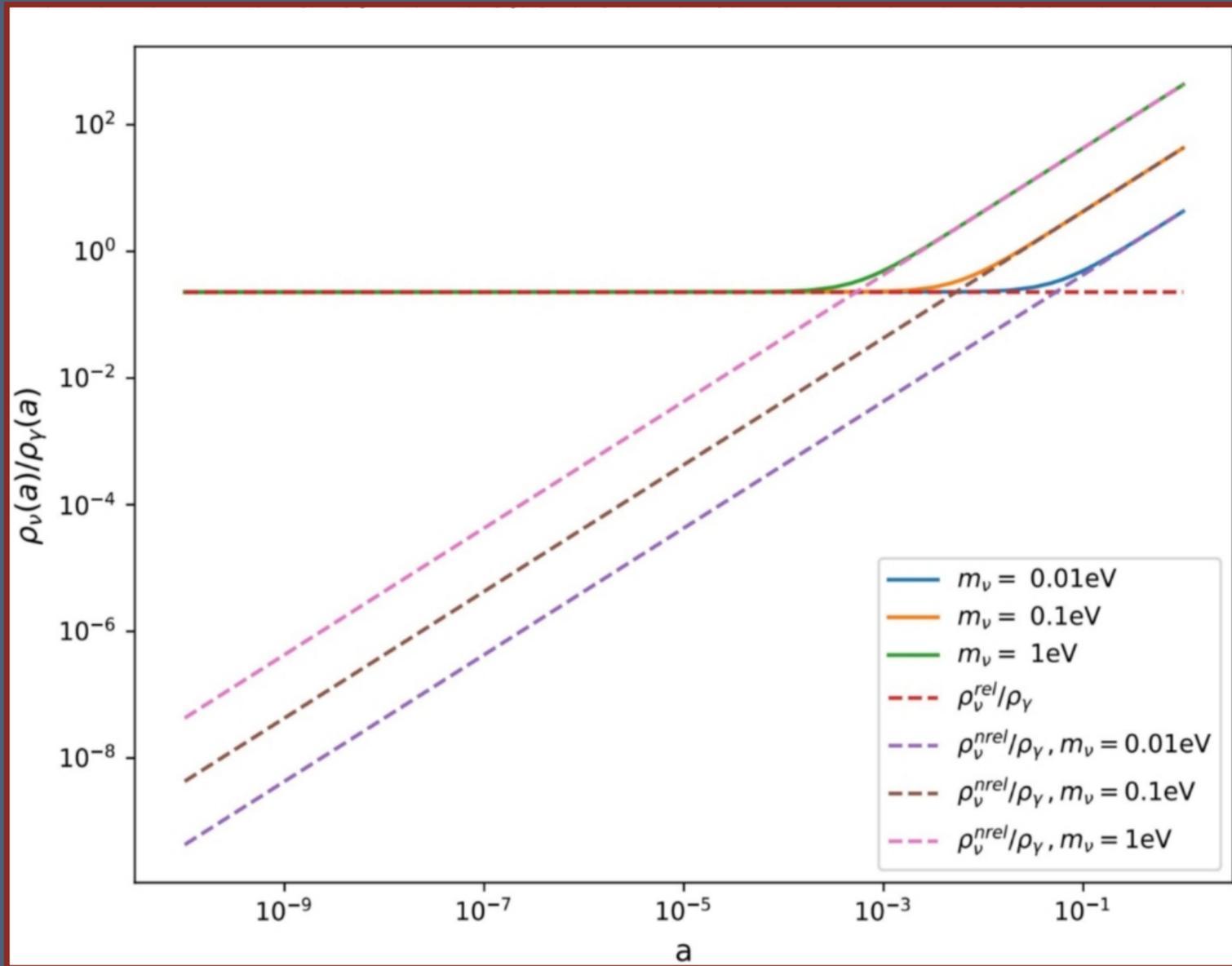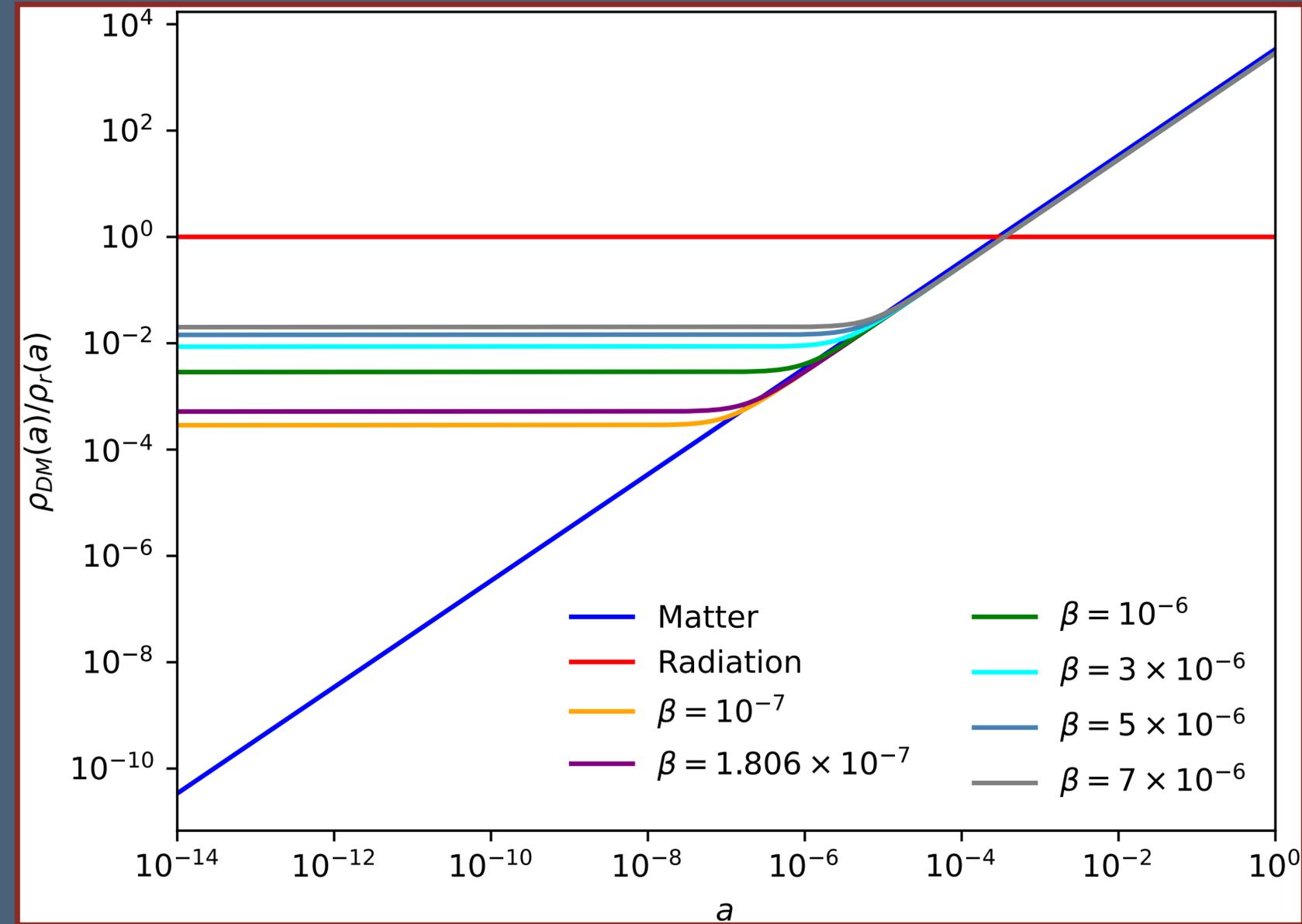
Cosmological evolution of the EoS
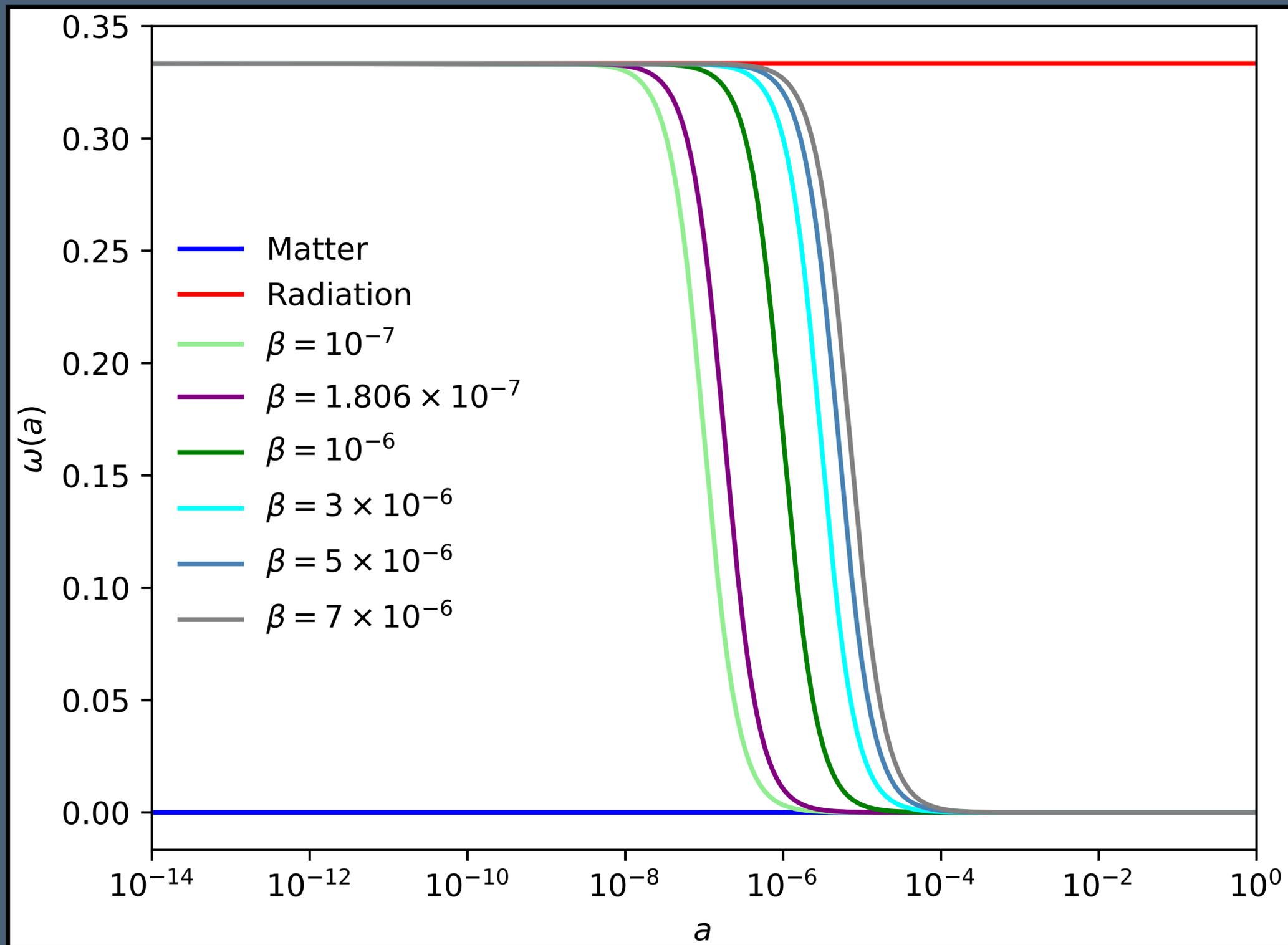
$$\omega_{DM}(a) \equiv \frac{1}{3}\frac{\beta^2}{a^2 + \beta^2}.$$

$$\omega_{DM} = \begin{cases} 1/3 & \text{for } a \to 0 \\ 0 & \text{for } a \to \infty \end{cases}$$

Linear perturbations
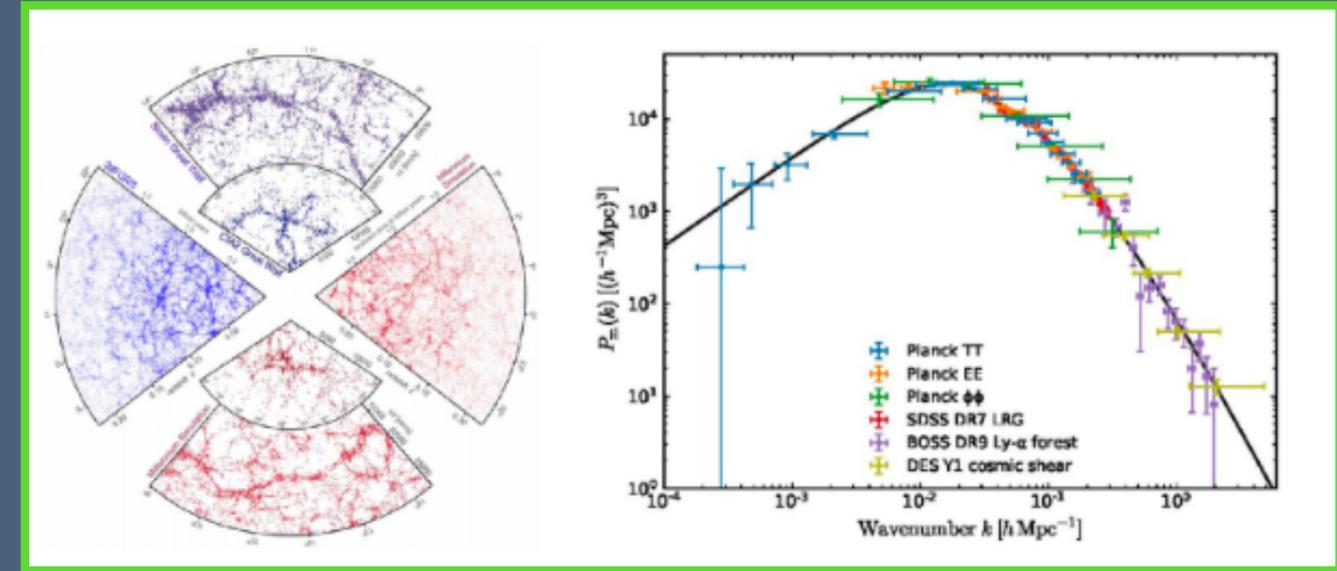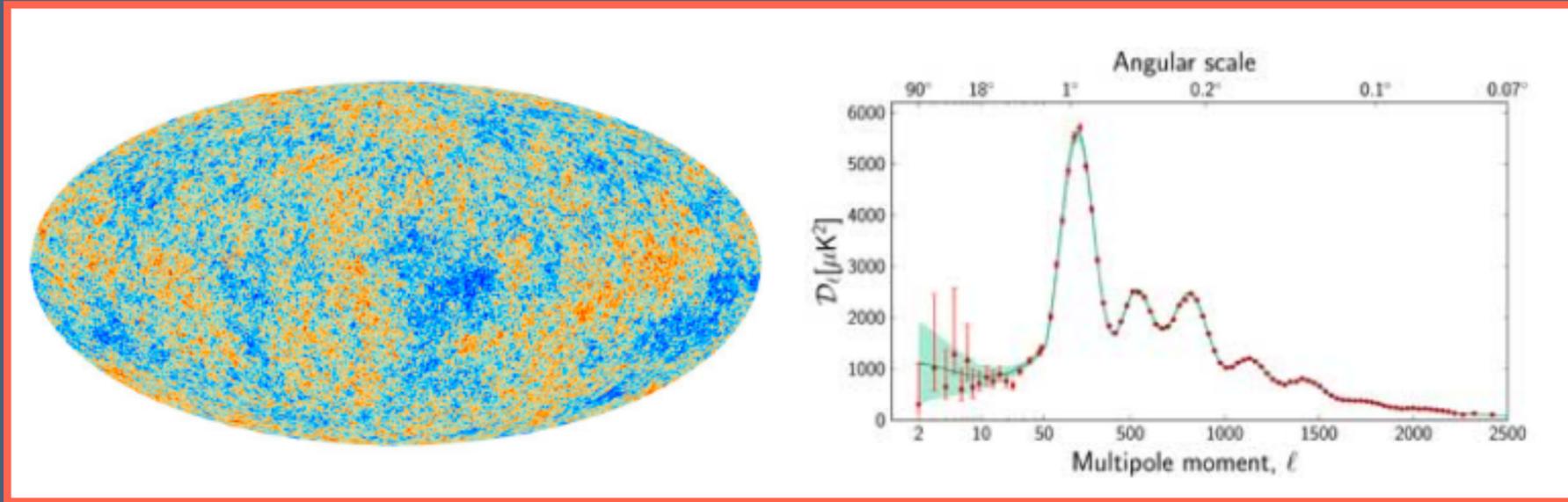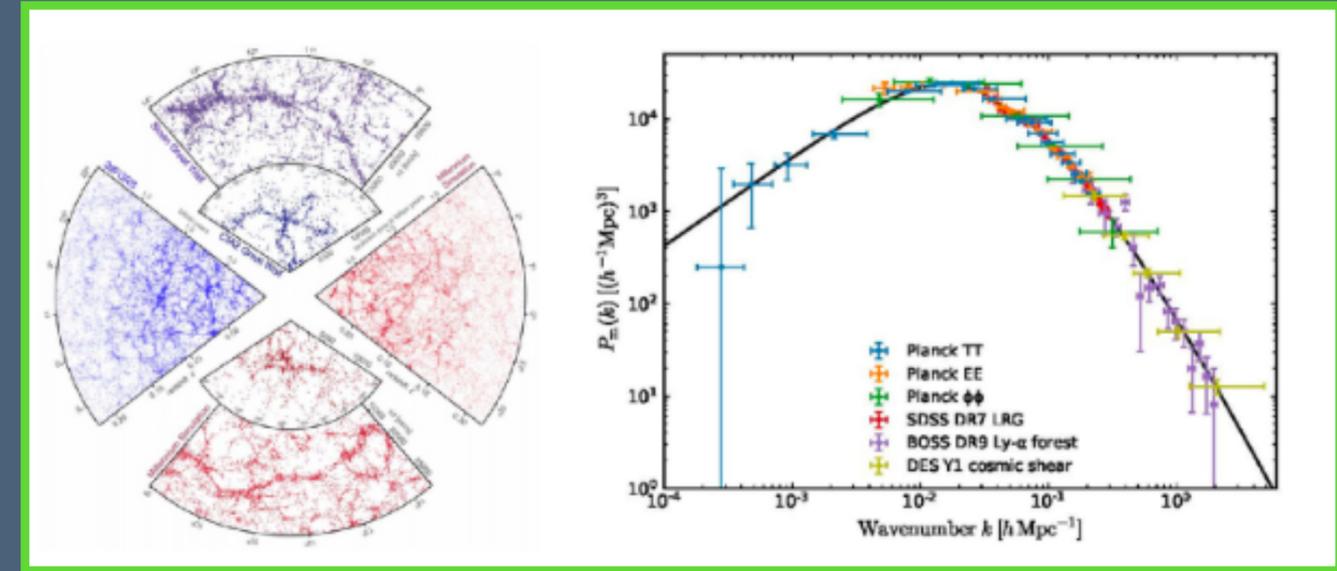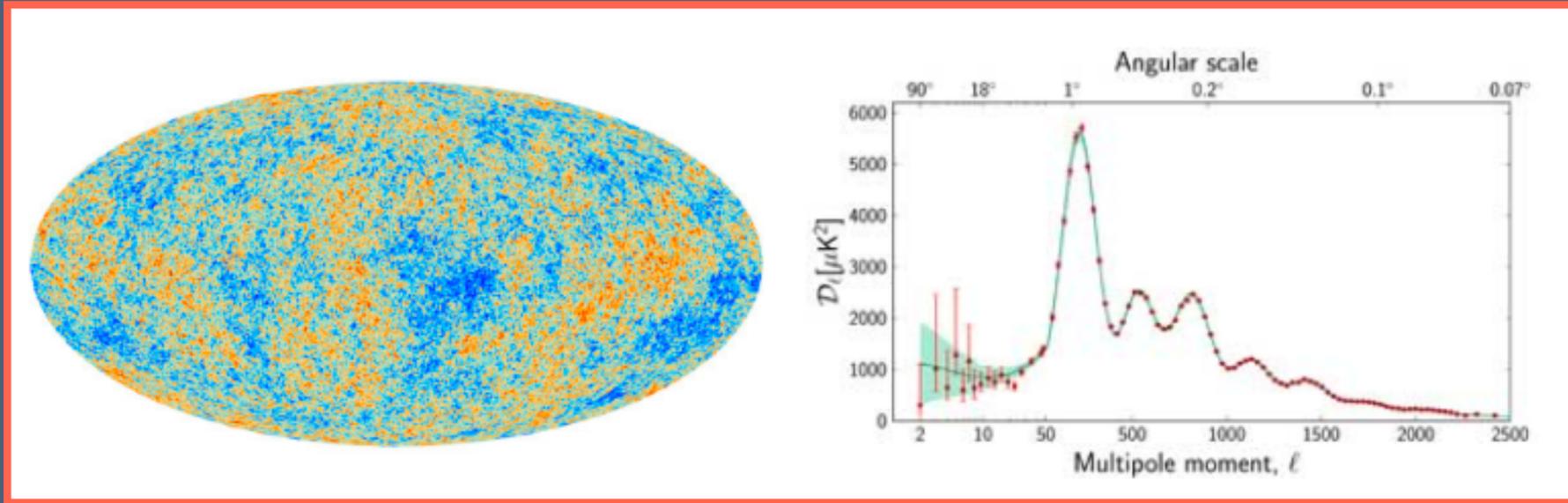
Linear perturbations
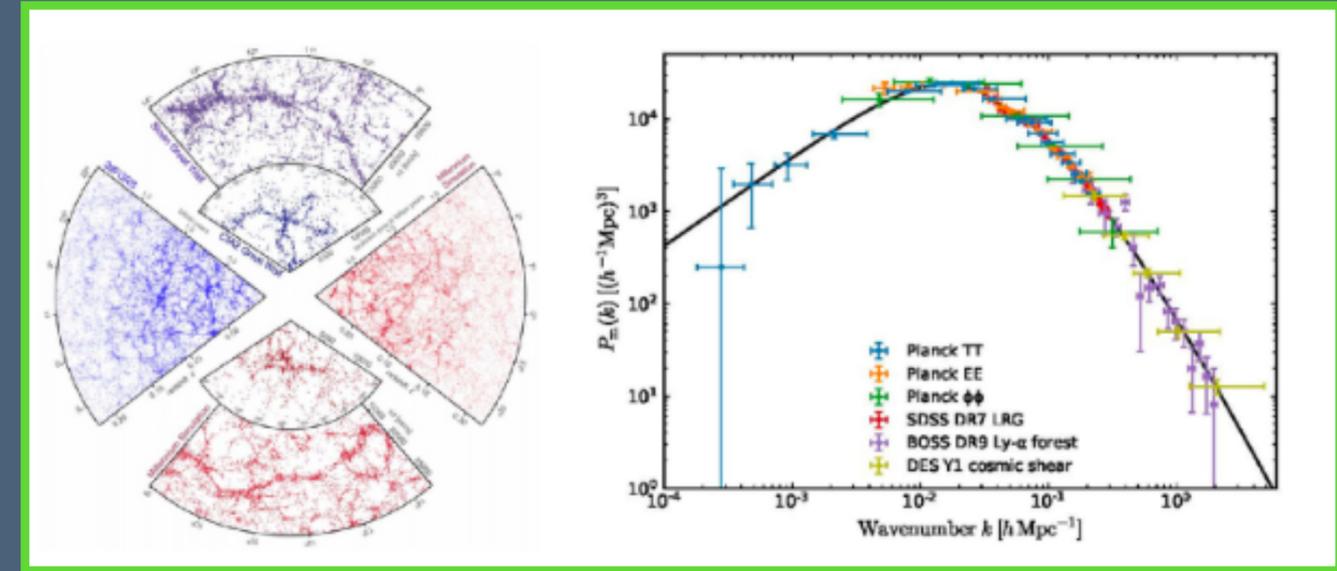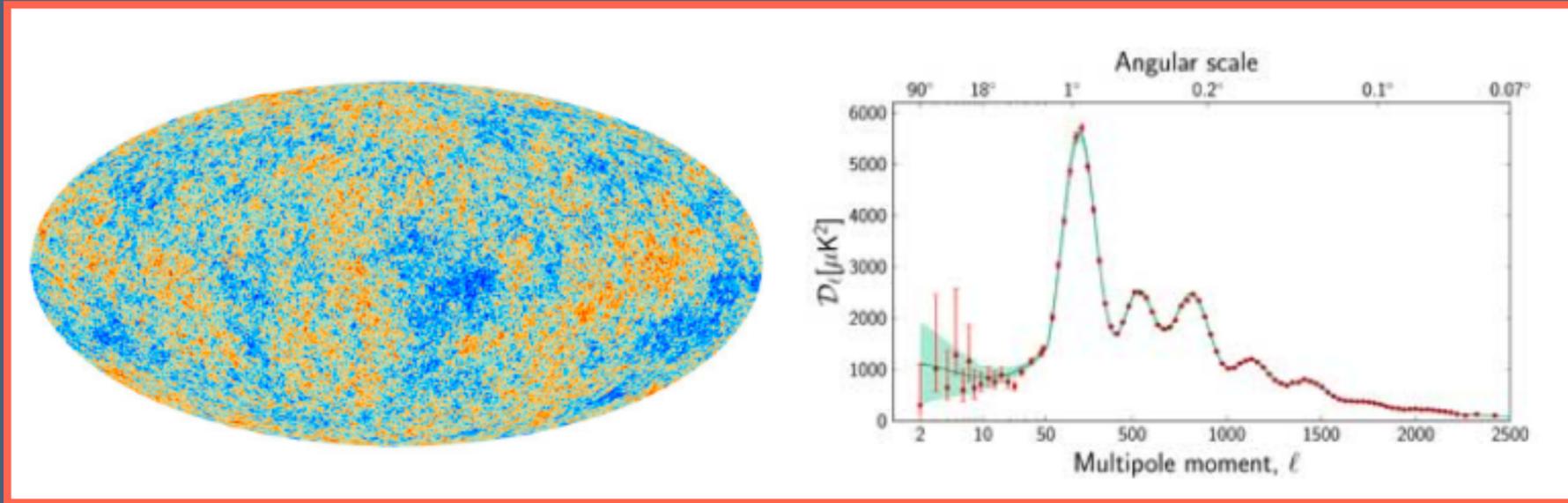
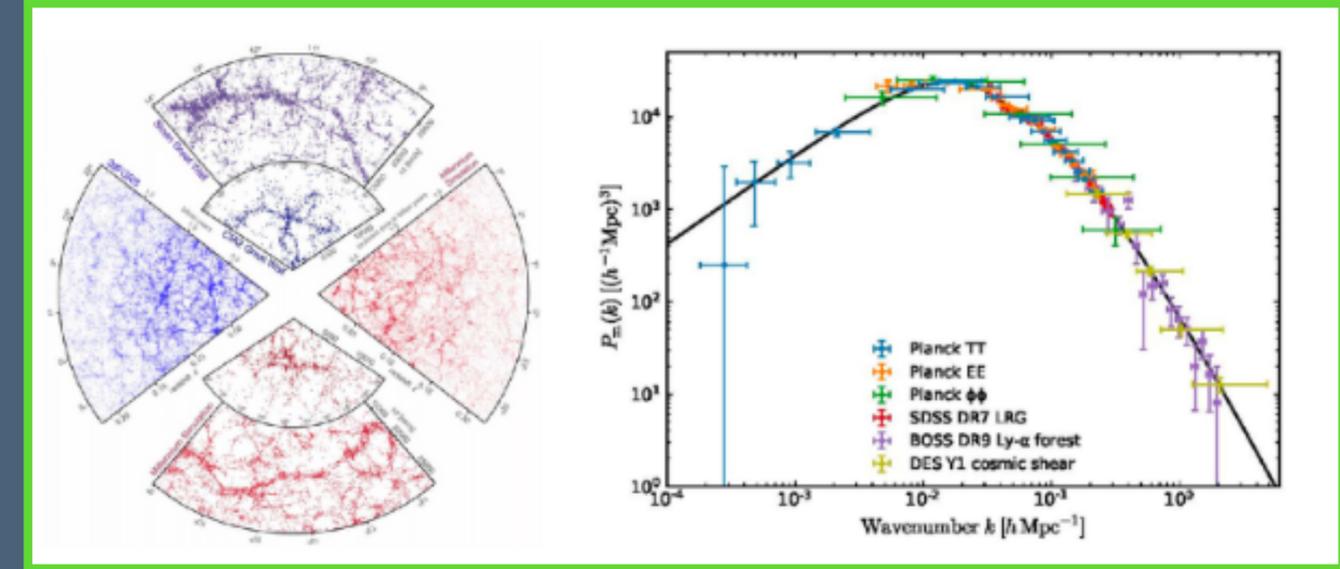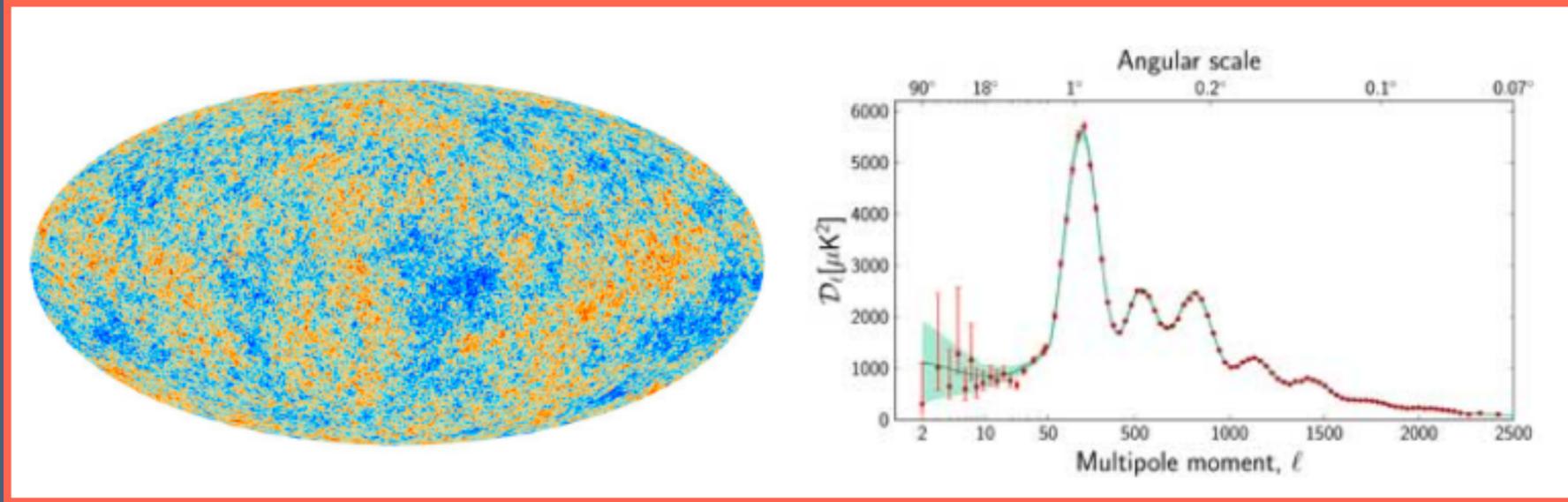Newtonian Gauge: $ds^2 = a^2(\eta)\left[-(1 + 2\psi)d\eta^2 + (1 - 2\phi)dx^i dx^j\right]$

Linear perturbations

Newtonian Gauge: $ds^2 = a^2(\eta)\left[-(1 + 2\psi)d\eta^2 + (1 - 2\phi)dx^i dx^j\right]$

$$\delta' = -(1 + \omega)\left(\theta - 3\phi'\right) - 3\frac{a'}{a}\left(c_s^2 - \omega\right)\delta\,, \qquad \theta' = \frac{a'}{a}(1 - 3\omega)\theta - \frac{\omega'}{1 + \omega}\theta + \frac{c_s^2}{1 + \omega}k^2\delta - k^2\sigma + k^2\psi\,.$$

Linear perturbations

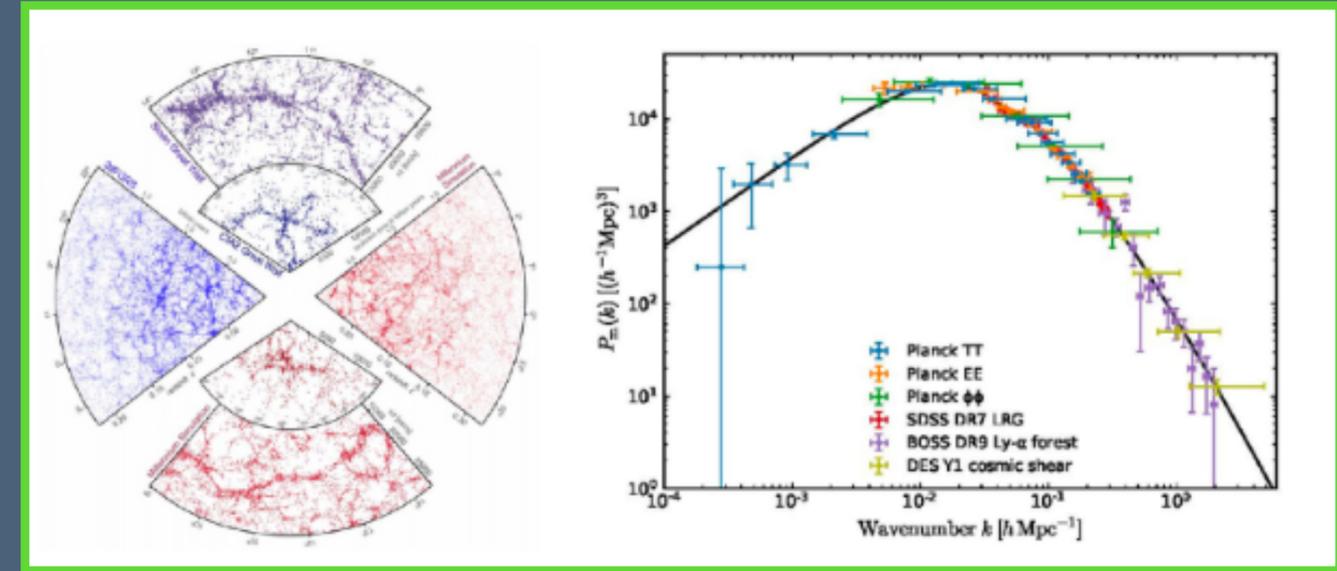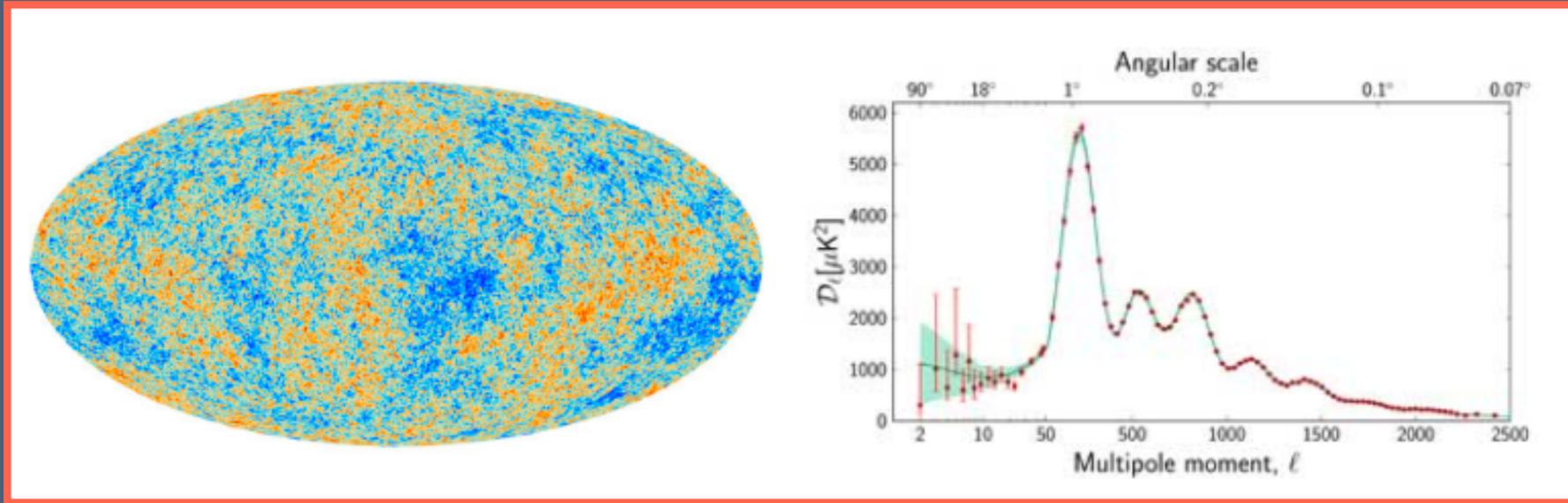Newtonian Gauge: $\quad ds^2 = a^2(\eta)\left[-(1+2\psi)d\eta^2 + (1-2\phi)dx^i dx^j\right]$

$$\delta' = -(1+\omega)\left(\theta - 3\phi'\right) - 3\frac{a'}{a}\left(c_s^2 - \omega\right)\delta, \qquad \theta' = \frac{a'}{a}(1-3\omega)\theta - \frac{\omega'}{1+\omega}\theta + \frac{c_s^2}{1+\omega}k^2\delta - k^2\sigma + k^2\psi.$$

For the Kinetic Gas Dark Matter we have:

$$\delta' = -(1+\omega)\left(\theta - 3\phi'\right) - 3\frac{a'}{a}\left(c_s^2 - \omega\right)\delta,$$

$$\theta' = -\frac{a'}{a}(1-3\omega)\theta - \frac{\omega'}{1+\omega}\theta + \frac{c_s^2}{1+\omega}k^2\delta + k^2\psi.$$

Linear perturbations

Newtonian Gauge: $ds^2 = a^2(\eta)\left[-(1 + 2\psi)d\eta^2 + (1 - 2\phi)dx^i dx^j\right]$

$$\delta' = -(1 + \omega)\left(\theta - 3\phi'\right) - 3\frac{a'}{a}\left(c_s^2 - \omega\right)\delta, \qquad \theta' = \frac{a'}{a}(1 - 3\omega)\theta - \frac{\omega'}{1 + \omega}\theta + \frac{c_s^2}{1 + \omega}k^2\delta - k^2\sigma + k^2\psi.$$
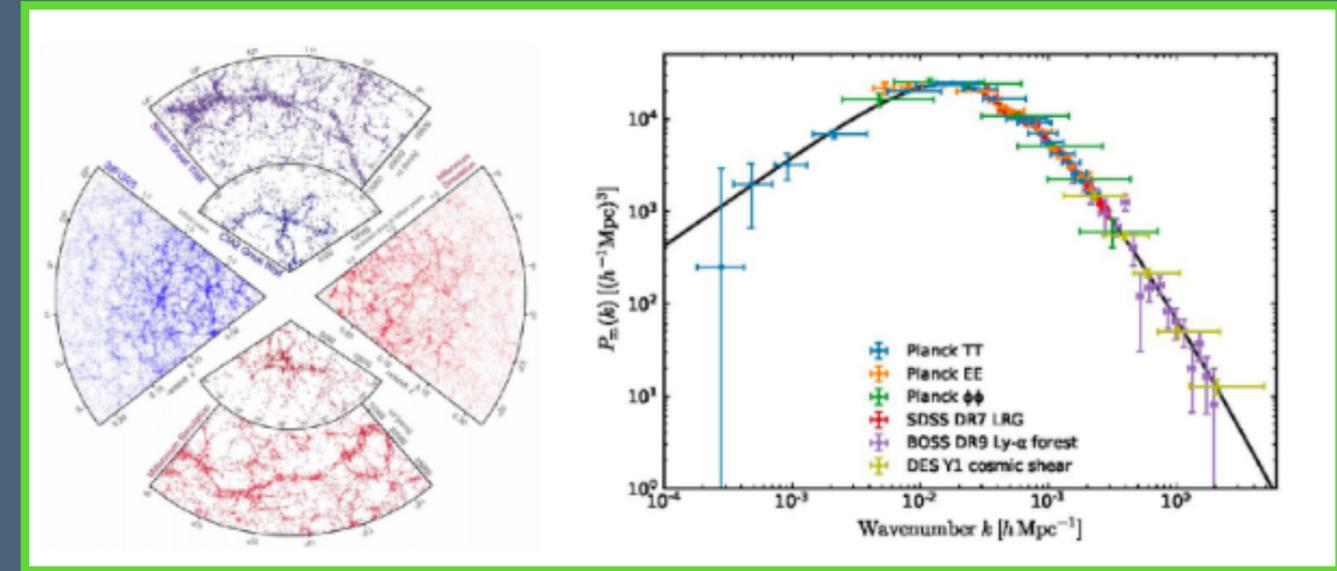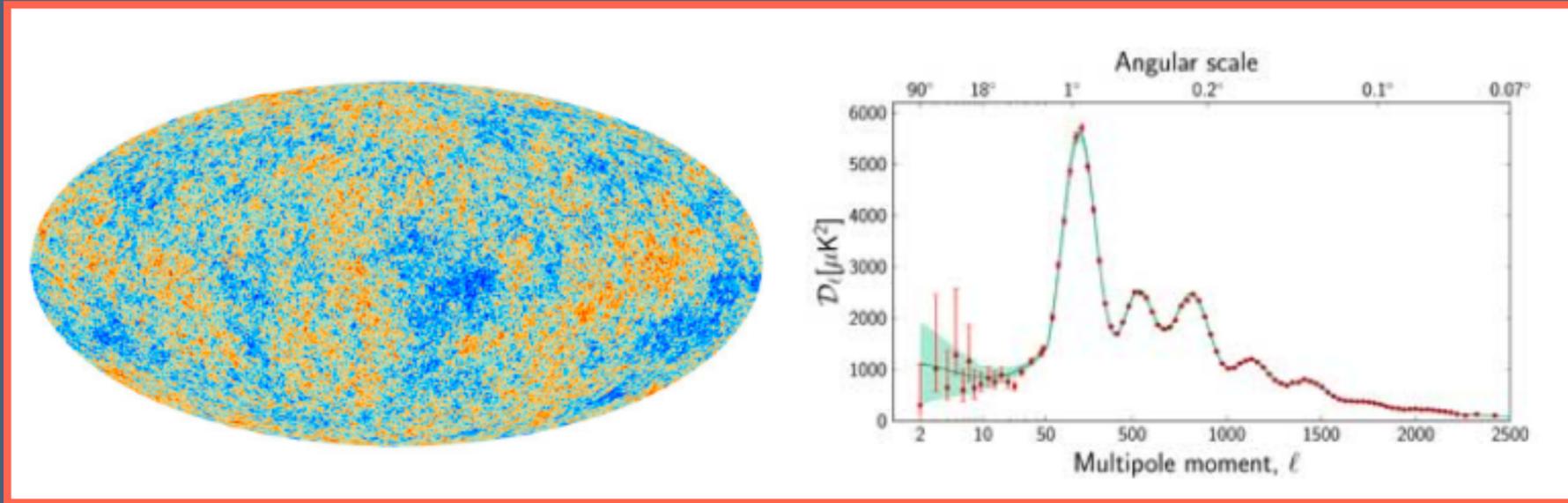
For the Kinetic Gas Dark Matter we have:

$$c_s^2(a) = \omega(a)\left(\frac{4\beta^2 + 5a^2}{4\beta^2 + 3a^2}\right)$$

$$\delta' = -(1 + \omega)\left(\theta - 3\phi'\right) - 3\frac{a'}{a}\left(c_s^2 - \omega\right)\delta,$$

$$\theta' = -\frac{a'}{a}(1 - 3\omega)\theta - \frac{\omega'}{1 + \omega}\theta + \frac{c_s^2}{1 + \omega}k^2\delta + k^2\psi.$$
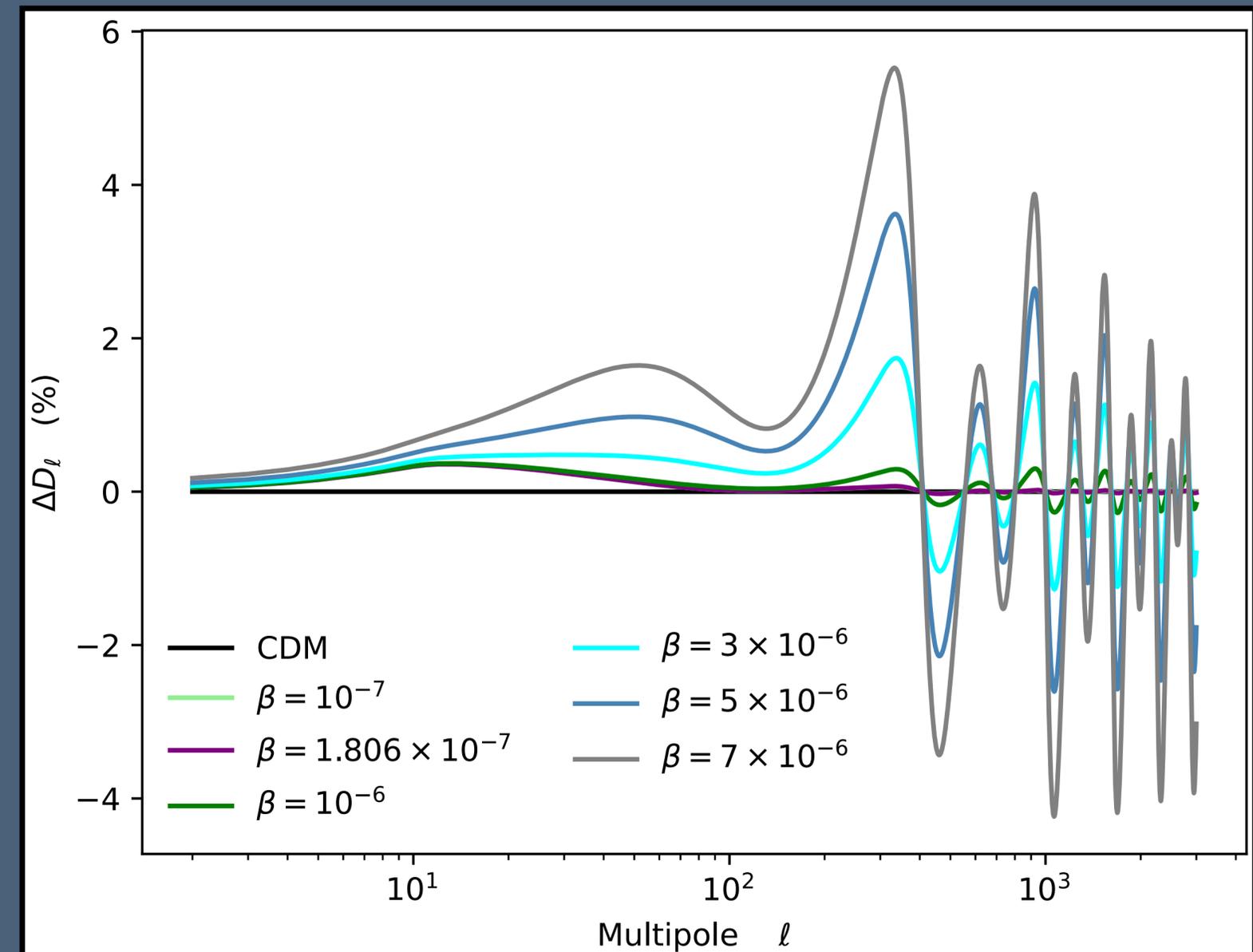
Linear perturbations

Newtonian Gauge:
$$ds^2 = a^2(\eta)\left[-(1 + 2\psi)d\eta^2 + (1 - 2\phi)dx^i dx^j\right]$$

$$\delta' = -(1 + \omega)\left(\theta - 3\phi'\right) - 3\frac{a'}{a}\left(c_s^2 - \omega\right)\delta, \qquad \theta' = \frac{a'}{a}(1 - 3\omega)\theta - \frac{\omega'}{1 + \omega}\theta + \frac{c_s^2}{1 + \omega}k^2\delta - k^2\sigma + k^2\psi.$$

For the Kinetic Gas Dark Matter we have:

$$c_s^2(a) = \omega(a)\left(\frac{4\beta^2 + 5a^2}{4\beta^2 + 3a^2}\right)$$

$$\delta' = -(1 + \omega)\left(\theta - 3\phi'\right) - 3\frac{a'}{a}\left(c_s^2 - \omega\right)\delta,$$

$$\theta' = -\frac{a'}{a}(1 - 3\omega)\theta - \frac{\omega'}{1 + \omega}\theta + \frac{c_s^2}{1 + \omega}k^2\delta + k^2\psi.$$
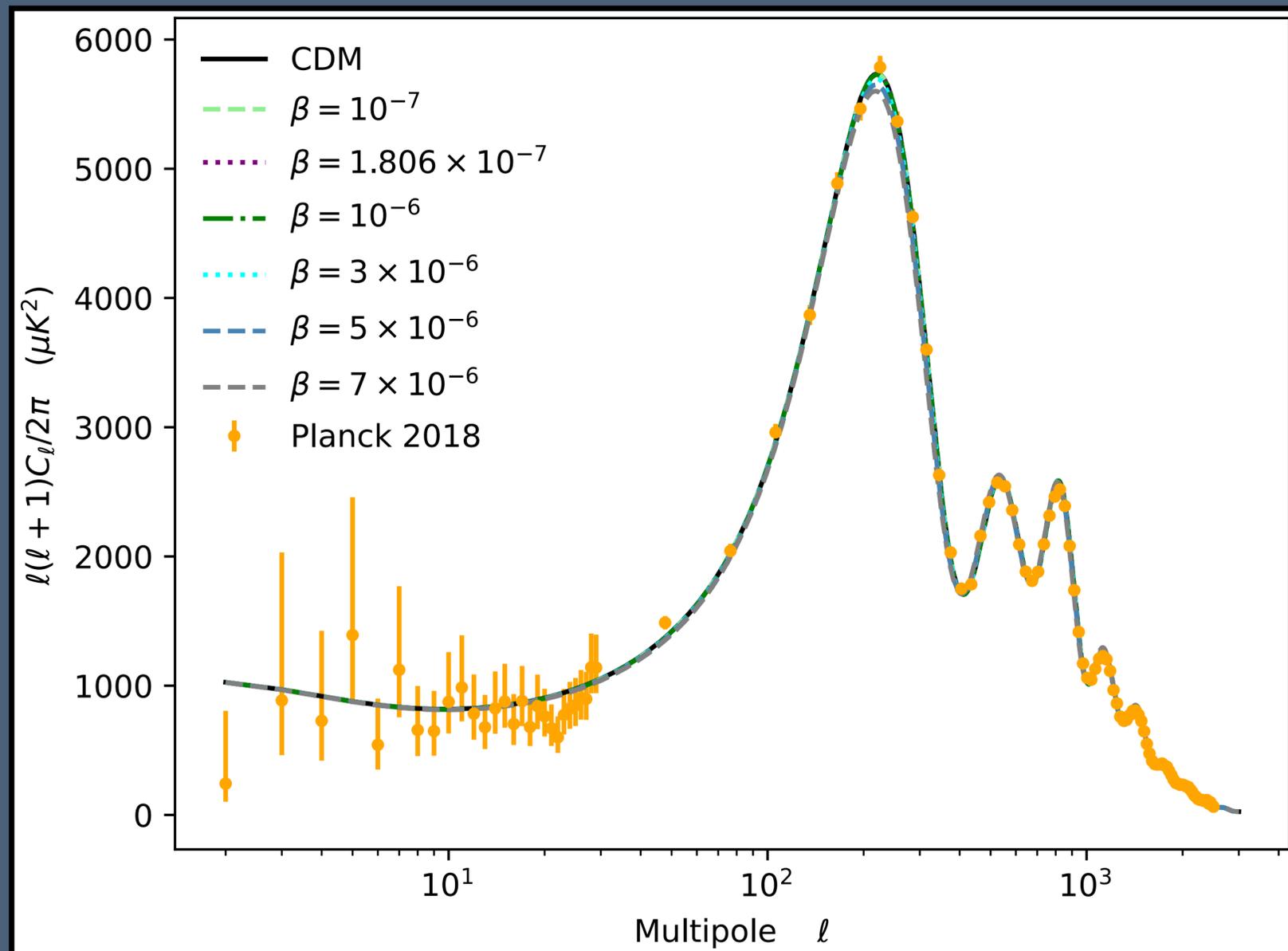
CDM

$$\delta' = -\left(\theta - 3\phi'\right),$$

$$\theta' = -\frac{a'}{a}\theta + k^2\psi.$$

Cosmological Observables

Numerical solutions for the CMB temperature anisotropies (left) and the matter power spectrum (right). Numerical solution with Boltzmann solver CLASS.

https://www.cosmos.esa.int/web/planck
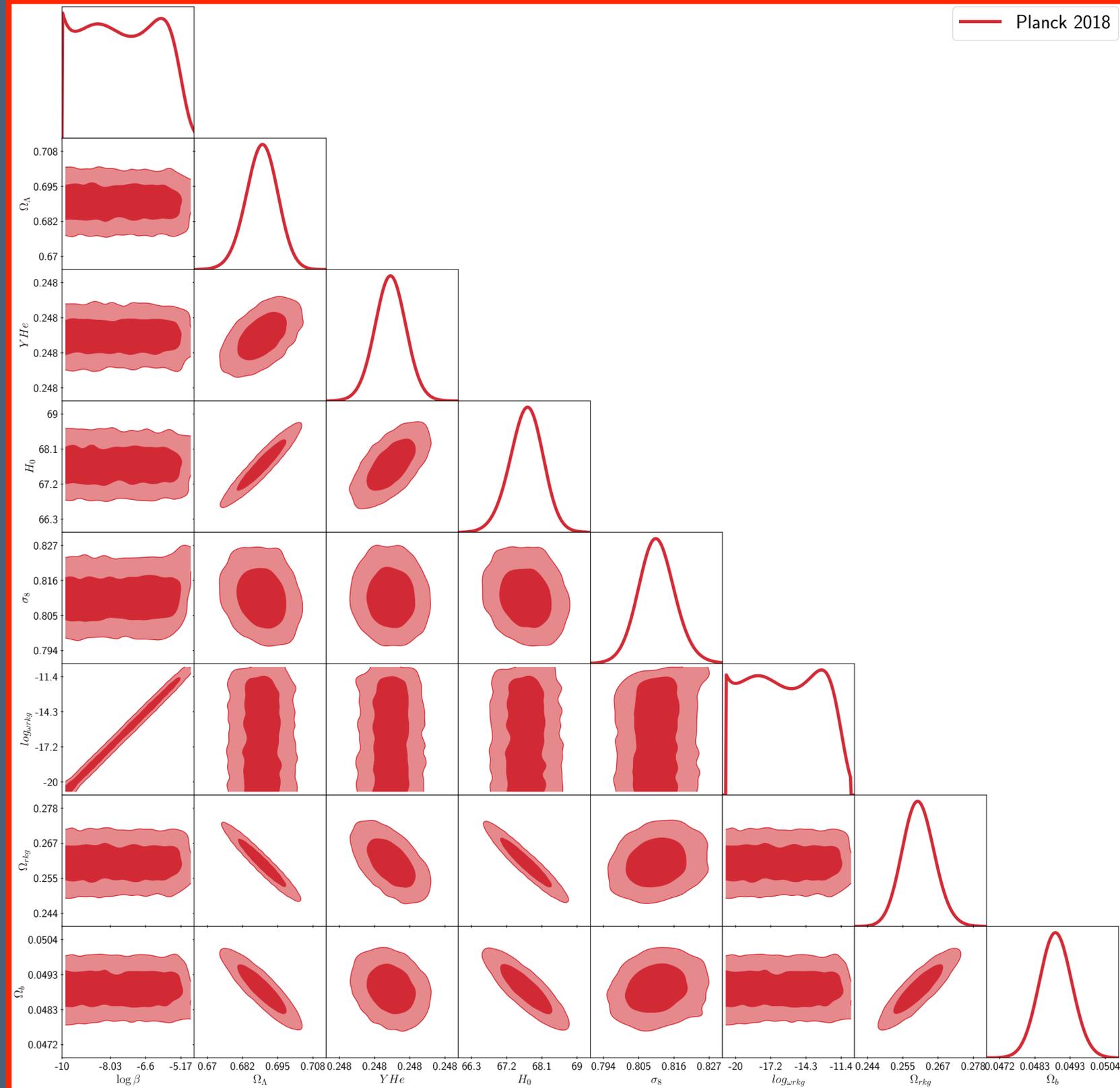
Cosmological Observables

Numerical solutions for the CMB temperature anisotropies (left) and the matter power spectrum (right). Numerical solution with Boltzmann solver CLASS.
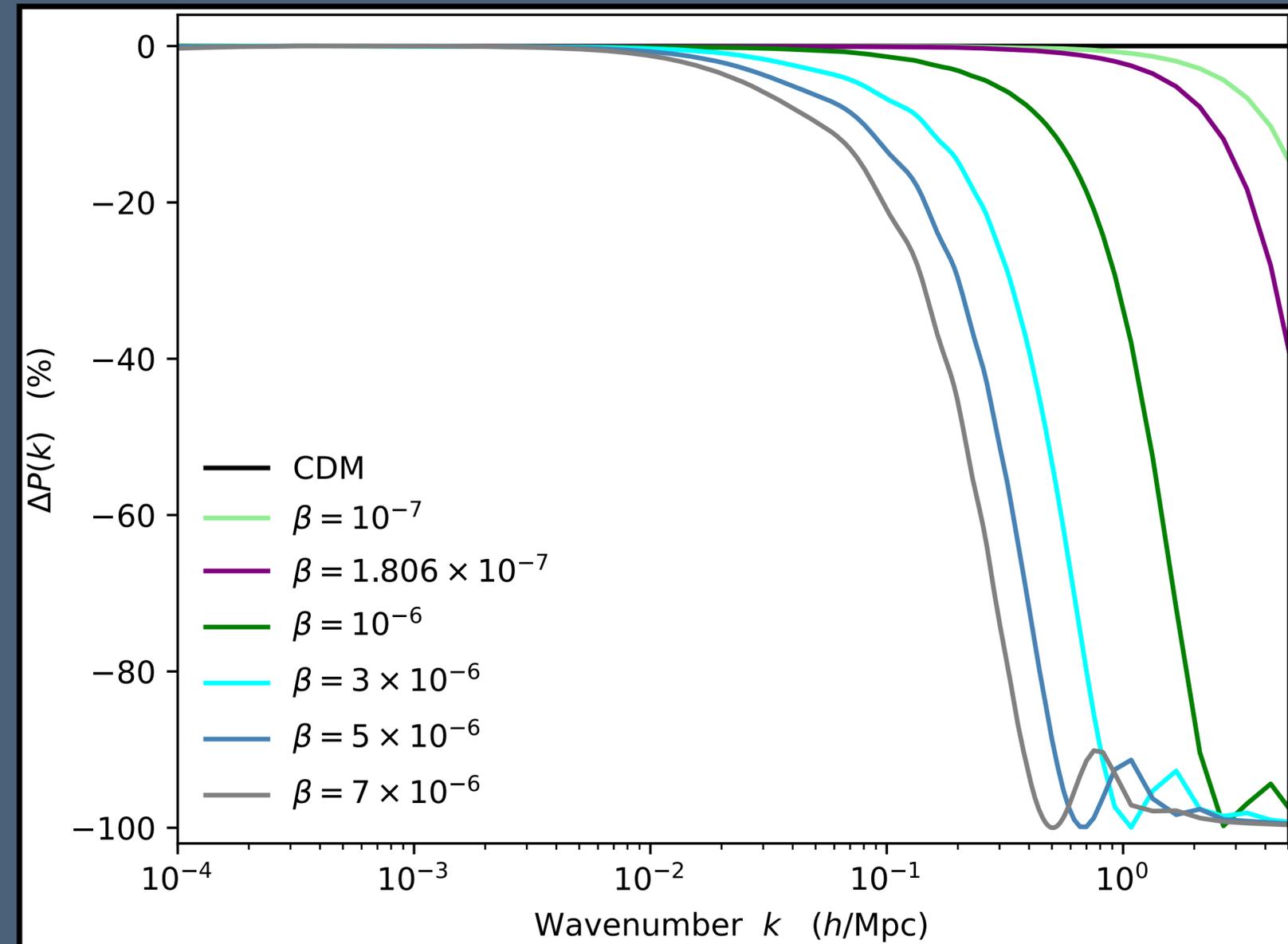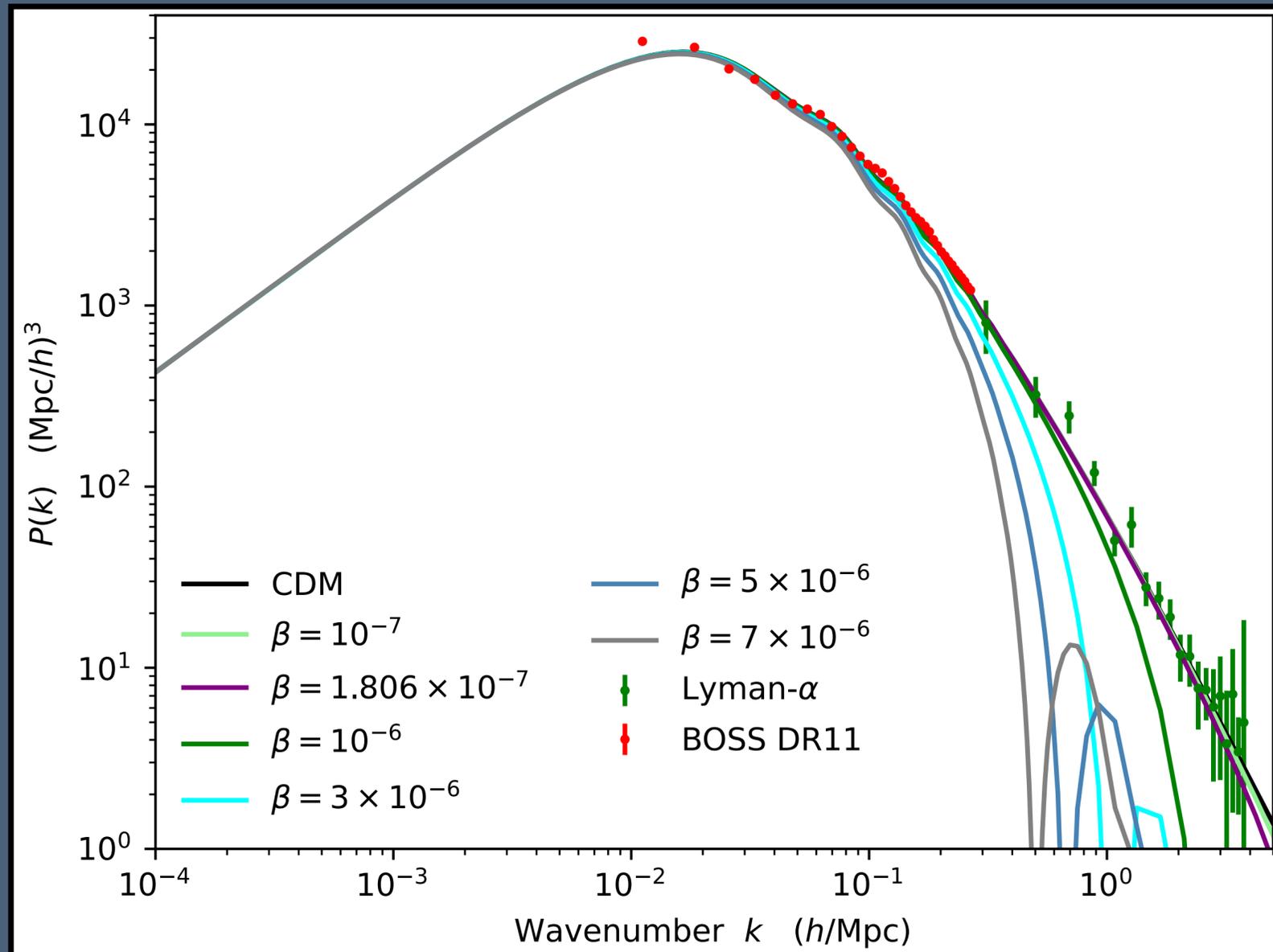
Statistical Constraints (CMB data)
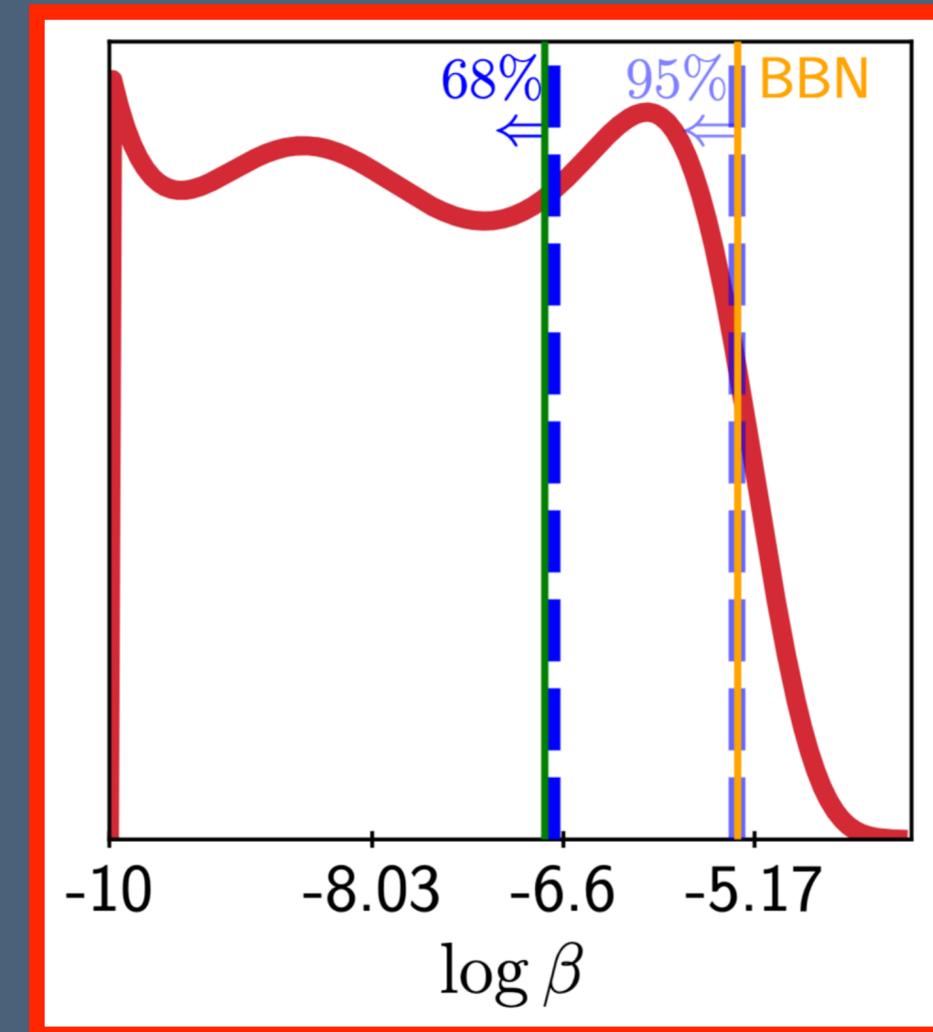
$$\log \beta < -6.6890 \pm 0.0031 \quad (68\% \text{ credibility}),$$
$$\log \beta < -5.3054 \pm 0.0020 \quad (95\% \text{ credibility}).$$

$$\beta \lesssim 1.806 \times 10^{-7} \quad \textbf{arXiv:1309.6971}$$
$$\beta \lesssim 4.89 \times 10^{-6} \quad \textbf{This work}$$

Statistical Constraints (Lyman-α data)
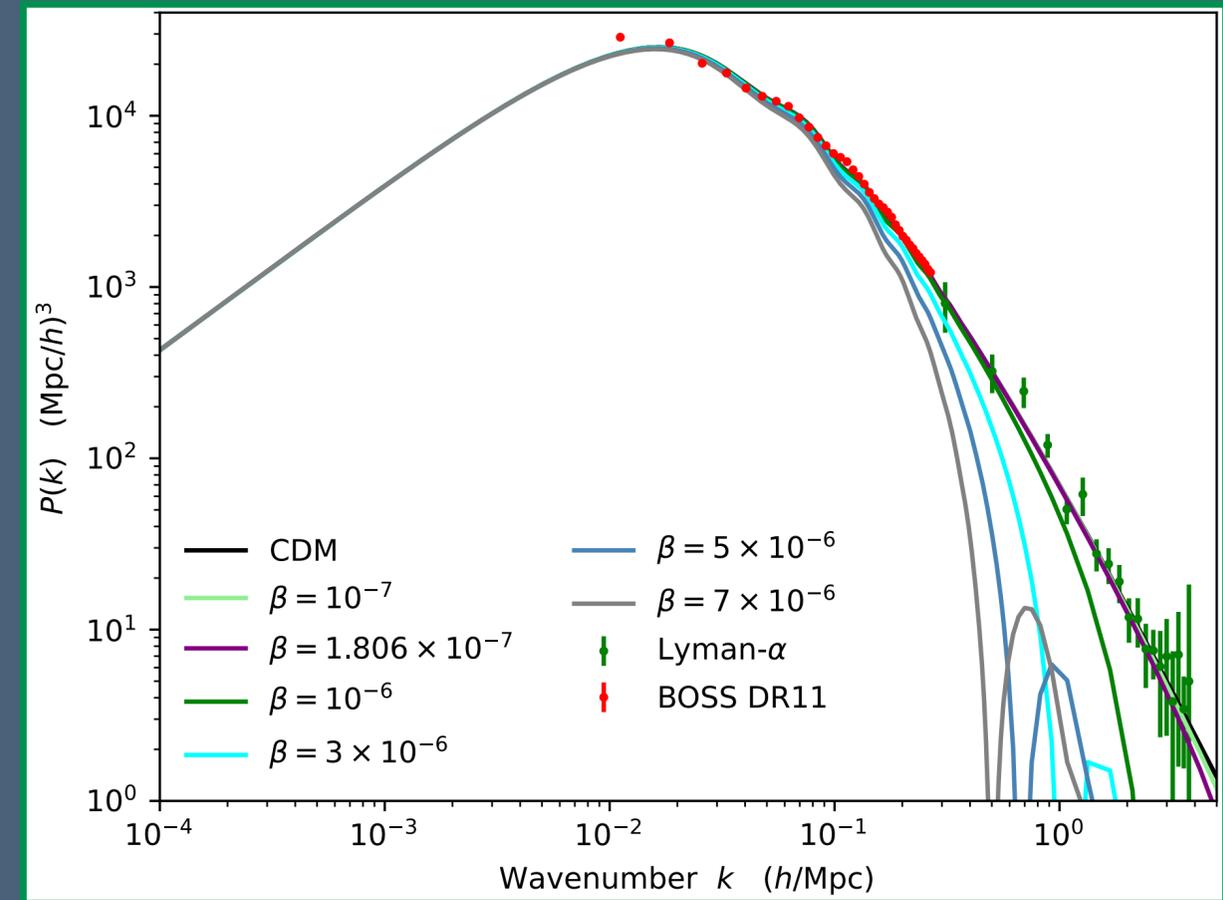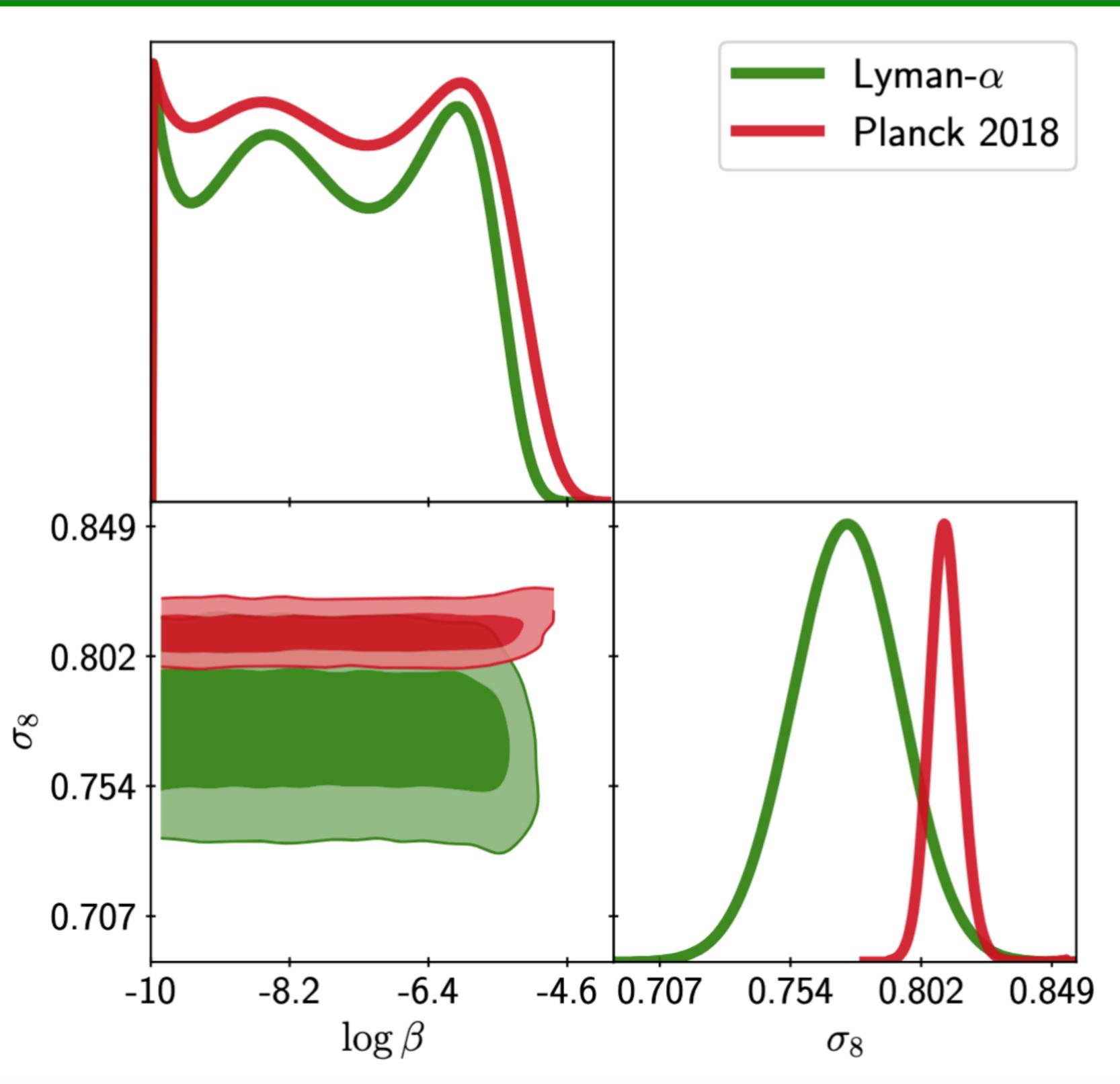
$$\log \beta < -6.8828 \pm 0.0027 \quad (68\% \text{ C.L.}),$$

$$\log \beta < -5.5596 \pm 0.0016 \quad (95\% \text{ C.L.}).$$

Final remarks and work in progress

○ From a geometric approach, it is possible to build the distribution function for the dark matter component. This is possible within the formalism of *Covariant Kinetic Theory of Relativistic Gases*.

○ Under this framework, the dark matter component behaves as radiation at early times and as dust at late times.

○ Statistical analysis put upper bounds on the only free parameter β, which in terms of the velocity of the gas it translates to:

$$|\vec{v}_0| \lesssim 61.4 \pm 0.4 \ \mathrm{m/s} \quad (68\% \ \mathrm{credibility}) \, .$$

$$|\vec{v}_0| \lesssim 1{,}484 \pm 6.8 \ \mathrm{m/s} \quad (95\% \ \mathrm{credibility}) \, .$$

○ Ongoing work is focused on the development of perturbations of the distribution function.

Thanks for your attention

Contact: <u>francisco.linares@umich.mx</u>